1   Coordination of genome replication and anaphase entry by rDNA copy number in *S. cerevisiae*

2

3   Elizabeth X. Kwan, Gina M. Alvino, Kelsey L. Lynch, Paula F. Levan, Haley M. Amemiya,

4   Xiaobin S. Wang, Sarah A. Johnson, Joseph C. Sanchez, Madison A. Miller, Mackenzie Croy,

5   Seung-been Lee, Maria Naushab, Josh T. Cuperus, Bonita J. Brewer, Christine Queitsch*, and

6   M. K. Raghuraman*

7

8   Department of Genome Sciences; University of Washington; Seattle, Washington, 98195; United

9   States of America

10

11   *Corresponding authors (queitsch @ u.washington.edu; raghu @ u.washington.edu)

12   Further information and requests for resources and reagents should be directed to and will be

13   fulfilled by M. K. Raghuraman (raghu @ u.washington.edu)

14

15   **ABSTRACT**

16   Eukaryotes maintain hundreds of copies of ribosomal DNA (rDNA), many more than

17   required for ribosome biogenesis, suggesting a yet undefined role for large rDNA arrays outside

18   of ribosomal RNA synthesis. We demonstrate that reducing the *Saccharomyces cerevisiae* rDNA

19   array to 35 copies, which is sufficient for ribosome function, shifts rDNA from being the latest

20   replicating region in the genome to one of the earliest. This change in replication timing results

21   in delayed genome-wide replication and classic replication defects. We present evidence that the

22   requirement for rDNA to replicate late, which is conserved among eukaryotes, also coordinates

23   the completion of genome replication with anaphase entry through the proper sequestration of

24   the mitotic exit regulator Cdc14p in the rDNA-containing nucleolus. Our findings suggest that,

25   instead of being a passive repetitive element, the large late-replicating rDNA array plays an

26   active role in genome replication and cell cycle control.

27

28   Keywords: rDNA, ribosomal DNA, replication, genome, Cdc14, Fob1, replication time,

29   anaphase

30

31 **INTRODUCTION**:

32   Ribosomal DNA (rDNA) is uniquely situated at the intersection of ribosome biogenesis

33 and genome replication, fundamental processes required for cell growth and proliferation. The

34 rDNA sequence is comprised of four ribosomal RNA genes, which encode the core components

35 of the ribosome; multiple rDNA copies are arranged in tandem to form large arrays. Many

36 species have hundreds of rDNA copies per haploid genome: *e.g.,* 90-300 in *Saccharomyces*

37 *cerevisiae*, 70-400 in *Caenorhabditis elegans*, 80-600 in *Drosophila melanogaster,* 500-2500 in

38 *Arabidopsis thaliana*, and 30-800 in humans (Mohan and Ritossa, 1970; Morton et al., 2020;

39 Parks et al., 2018; Thompson et al., 2013). As the high rDNA copy number is often in

40 substantial excess of what is required to meet ribosome demands, the majority of rDNA repeats

41 are silenced (Conconi et al., 1992, 1989; Dammann et al., 1993; French et al., 2003; McStay and

42 Grummt, 2008; Ye and Eickbush, 2006). Nevertheless, active maintenance of seemingly

43 overabundant rDNA copies is conserved (Nelson et al., 2019), hinting that high rDNA copy

44 number may have roles beyond ribosome production.

45   The phenotypic consequences of rDNA copy number variation span a broad range of

46 cellular processes. While ribosome deficiencies result when rDNA copy number drops below a

47 certain threshold (Delany et al., 1994; French et al., 2003; Ritossa and Atwood, 1966; Sanchez et

48 al., 2017), other phenotypes result from rDNA copy number variants that are sufficient for

49 ribosome biogenesis (Gibbons et al., 2014; Ide et al., 2010; Lu et al., 2018; Michel et al., 2005;

50 Paredes et al., 2011; Picart-Picolo et al., 2020; Wang and Lemos, 2017; Xu et al., 2017).

51 Additionally, the plastic nature of the rDNA locus allows copy number fluctuations in the face of

52 stresses such as nutrient availability (Aldrich and Maggert, 2015) or replication defects (Ide et

53 al., 2007; Lynch et al., 2019; Salim et al., 2017; Sanchez et al., 2017). Because rDNA copy

54 number changes often occur in response to various forms of replication stress, we sought to ask

55 whether the reverse is also true: does rDNA copy number variation impact genome stability by

56 influencing genome replication?

57   Given the vast length of the highly repetitive rDNA arrays, replication initiation must

58 occur within the rDNA sequence, as documented in several species (Bénard et al., 1995; Brewer

59 and Fangman, 1988; Coffman et al., 2006; Hyrien and Méchali, 1992; Little et al., 1993; López-

2

60   estraño et al., 1998). Extensive characterization in the budding yeast *S. cerevisiae* has shown

61   that each 9.1 kb repeat contains a potential origin of replication (rDNA Autonomously

62   Replicating Sequence or rARS, (Brewer et al., 1992; Miller and Kowalski, 1993)). For a wild

63   type yeast rDNA array of 150 copies, only 30-40 of the 150 replication origins are estimated to

64   initiate replication ("fire") within an S phase (Brewer and Fangman, 1988; Linskens and

65   Huberman, 1988). Genome-wide origin firing is limited by the low abundance of initiation

66   factors that promote the temporal staggering of origin activation (Collart et al., 2013; Lynch et

67   al., 2019; Mantiero et al., 2011; Yoshida et al., 2013). Hyperactivation of rDNA replication

68   diverts replication factors away from unique regions of the genome (Shyian et al., 2016; Yoshida

69   et al., 2014) and leads to persistent underreplication of certain genomic regions (Foss et al.,

70   2017). We reasoned that reduction of rDNA copy number from the wild type burden of 100-200

71   copies would alleviate the competition for limiting initiation factors at the other 300 replication

72   origins across the genome (Nieduszynski et al., 2007).

73   Here we assess genome replication in isogenic yeast strains with rDNA arrays that are

74   either wild type in size (100-180 copies) or minimal (35 copies). Contrary to our expectations,

75   we discovered that the minimal rDNA array does not reduce competition with non-rDNA

76   origins, but instead drastically advances rDNA replication time and increases the density of

77   active rDNA origins. The large burst of early rDNA initiations from the minimal rDNA array

78   causes a delay in replication in the rest of the genome. Furthermore, loss of the replication fork

79   barrier gene *FOB1* sensitizes minimal rDNA strains to DNA damage and premature exit into

80   anaphase, suggesting new roles for both Fob1p and rDNA in monitoring S phase progression.

81   These findings show that the rDNA array is not merely a passive repetitive element during

82   replication, but an active force that coordinates genome replication and cell cycle progression.

83

84   **RESULTS:**

85   <u>Strains with minimal rDNA arrays are not defective in ribosome production</u>

86   We generated isogenic strains with a reduced rDNA array at the endogenous rDNA locus

87   (Figure 1A) using the pRDN1-Hyg plasmid-based method (Chernoff et al., 1994; Kobayashi et

3

88   al., 2001; Kwan et al., 2013). About 20-25% of the isolates with rDNA reductions showed

89   increased ploidy (Figure S1A-B). Because maintenance of reduced rDNA requires the deletion

90   of *FOB1* to prevent rDNA recombination and expansion, we included both *FOB1* and *fob1Δ*

91   strains with wild type rDNA arrays as control strains. We also examined strains with weakened

92   rDNA origins (rDNA^{RM}) (Kwan et al., 2013), which we hypothesized would further reduce

93   rDNA replication initiation events and favor initiation at origins outside the rDNA locus. We

94   generated strains with 35, 45, and 55 copies of rDNA and decided to focus on strains with the

95   smallest rDNA array (minimal rDNA strains, 35 rDNA *fob1Δ* and 35 rDNA^{RM} *fob1Δ*) in

96   comparison and compared these strains to those with wild type copy number (170 rDNA, 180

97   rDNA *fob1Δ*, and 100 rDNA^{RM}).

98   Although previous work demonstrated that 35 rDNA copies are sufficient for wild type

99   levels of rRNA synthesis and ribosome biogenesis (Dauban et al., 2019; French et al., 2003; Ide

100 et al., 2010; Kim et al., 2006), we wanted to confirm the absence of ribosome biogenesis defects

101 in the minimal rDNA strains. We assessed phenotypes due to ribosome insufficiency: slower

102 growth rate, increased sensitivity to cycloheximide over a range of concentrations, and decreased

103 relative 25S rRNA abundance (Abovich et al., 1985; Rosado et al., 2007; Sanchez et al., 2017).

104 The minimal rDNA strains behaved similarly to the wild type rDNA controls in these assays

105 (Figure S1C-E), confirming that rDNA reduction to 35 rDNA copies does not generate

106 significant ribosome biogenesis defects.

107

108 <u>Minimal rDNA strains show reduced plasmid maintenance and increased sensitivity to MMS and</u>

109 <u>hydroxyurea</u>

110   We examined the effects of rDNA copy number reduction on plasmid maintenance, a

111 basic assay that identifies mutants with DNA replication defects on the basis of their poor ability

112 to replicate plasmids (Maine et al., 1984; Shima et al., 2007; Tye, 1999). Because replication

113 initiation at a plasmid origin is subject to the same competition for replication factors as genomic

114 origins, we expected that strains with minimal rDNA arrays would show improved plasmid

115 maintenance compared to the wild type rDNA controls. However, both minimal rDNA strains

116 displayed high loss rates of the *ARS1* (Autonomously Replicating Sequence 1, (Stinchcomb et

Figure 1. Strains with minimal rDNA copy number exhibit non-rDNA replication defects.
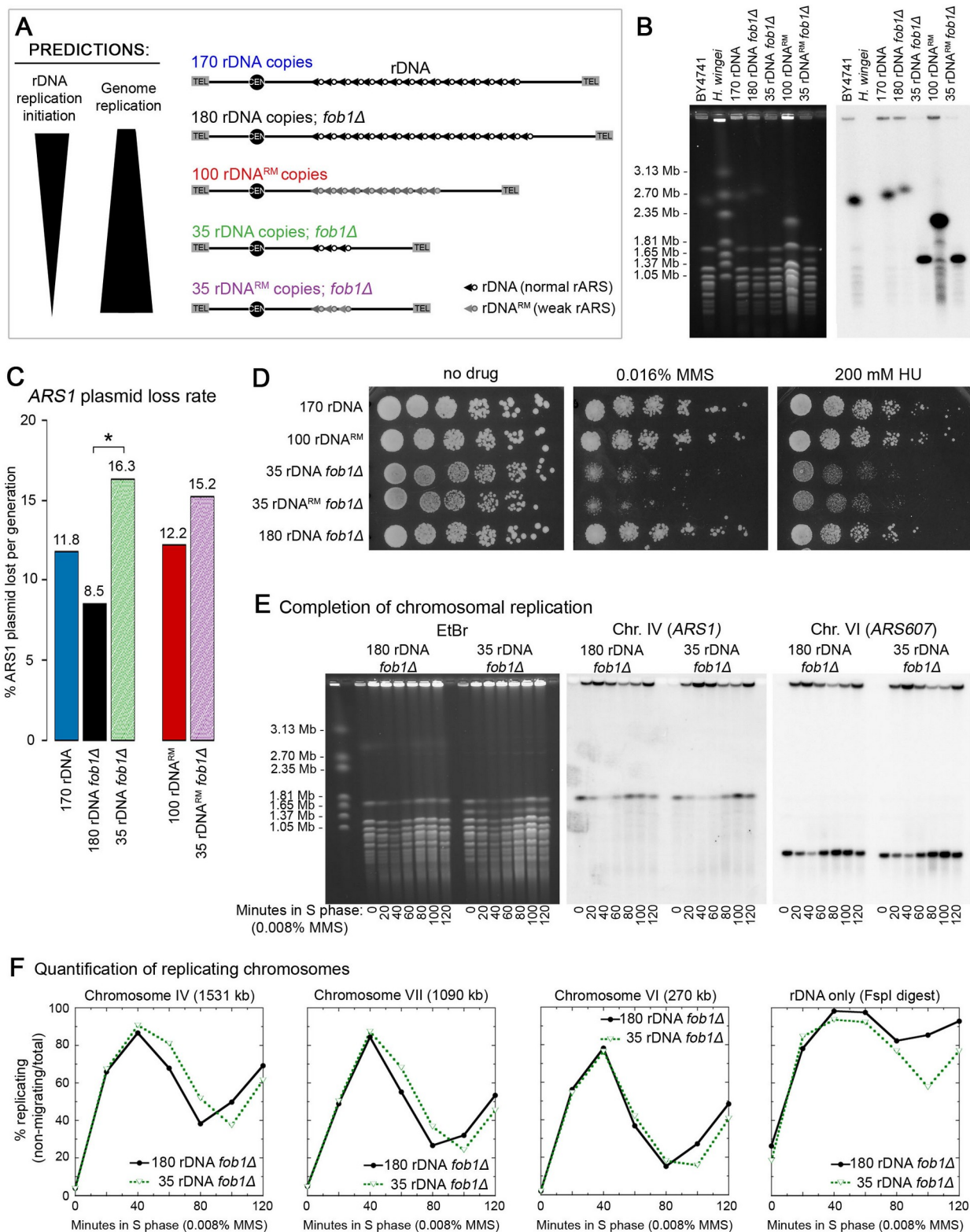
118 **Figure 1. Strains with minimal rDNA copy number exhibit non-rDNA replication defects.** (A)
119 Depiction of rDNA arrays examined in this study and prediction of genome replication effects resulting
120 from competition for replication factors. Strains differed at the rDNA locus in copy number and/or
121 presence of a weak rDNA origin (rDNA^{RM}). (B) CHEF gel confirmation of rDNA copy number.
122 Ethidium bromide stained gel (left) and the resulting Southern blot (right) hybridized with a single copy
123 Chr. XII probe (*CDC45*). (C) Loss of maintenance of an *ARS1*-containing plasmid was assessed in
124 exponentially grown cultures. (*) indicates significant difference in plasmid loss rate calculated from
125 slope variance (p = 0.03). (D) Spot assays for sensitivity to 200 mM HU and 0.016% MMS. (E)
126 Migration assay of chromosomes from cells released into S phase in the presence of 0.08% MMS using
127 CHEF gel electrophoresis and Southern blotting. Chromosomes are unable to migrate out of the
128 plug/well while replicating (Hennessy & Botstein 1991), allowing for quantification of replicating vs.
129 non-replicating chromosomes (fully replicated and unreplicated)by comparing the signal in the gel body
130 vs. plug/well. Hybridization to specific sequences allows examination of individual chromosomes, IV
131 and VI shown. (F) Quantification of the percentage of chromosomes undergoing replication in 0.008%
132 MMS: chromosomes VI, IV, and VII as well as the isolated rDNA array. Completion of chromosome
133 replication is reflected in the decrease of signal in the CHEF gel well.

134 _____

135 al., 1979)) test plasmid: 16.3%/generation for the minimal rDNA strain and 15.2%/generation for

136 the minimal rDNA^{RM} strain, almost double that of the control *fob1Δ* strain with wild type rDNA

137 (8.5%/generation, *p* = 0.03) and higher than either of the wild type rDNA *FOB1* strains

138 (11.8%/generation and 12.2%/generation, Figure 1C). Since the Southern blot method reflects

139 the amount of plasmid relative to genomic DNA sequences in the culture (Brewer and Fangman,

140 1994), the observed differences can be ascribed to differences in plasmid replication rather than

141 segregation. Counter to our prediction that rDNA reduction would improve DNA replication,

142 the strains with minimal rDNA arrays instead showed defects in plasmid replication.

143   If minimal rDNA arrays are associated with defects in DNA replication, the strains

144 carrying these arrays should be hypersensitive to conditions that induce replication stress and

145 DNA damage (Shimada et al., 2002; Trabold et al., 2005). Hydroxyurea (HU) induces

146 replication stress by inhibiting the production of dNTPs, which does not directly damage DNA

147 (Alvino et al., 2007) but slows cell cycle progression through activation of the replication

148 checkpoint (Santocanale and Diffley, 1998). In contrast, MMS is an alkylating agent that

149 induces DNA damage (Paulovich and Hartwell, 1995). Consistent with previous work (Ide et

150 al., 2010), strains with minimal rDNA showed greater sensitivity to DNA damage by MMS

151 (Figure 1D). We found that rDNA reduction also conferred greater sensitivity to HU, suggesting

152 that reducing rDNA copy number induces problems with both DNA replication and repair.

153

154   <u>A minimal rDNA strain shows delayed replication completion across multiple chromosomes</u>

155   To determine if rDNA reduction leads to chromosomal replication defects, we performed

156   an S phase specific CHEF gel electrophoresis assay on strains with wild type or minimal rDNA

157   copy number. In CHEF gel electrophoresis, chromosomes that are undergoing replication will

158   not migrate from the well (Hennessy et al., 1991; Lynch et al., 2019), while non-replicating

159   chromosomes, either those that are pre-replication or have completed replication, migrate into

160   the gel at their expected sizes. To measure replication completion for individual chromosomes,

161   we quantified the relative amount of Southern blot hybridization signal remaining in the well at

162   20-minute intervals across a synchronous S phase. For this assay, G1 synchronized cells were

163   released into S phase (Ide et al., 2010) and cell cycle progression was confirmed by flow

164   cytometry (Figure S2A-B).

165   We examined replication completion for several chromosomes of different lengths as

166   well as the rDNA array itself in *fob1Δ* strains with wild type or minimal rDNA. As expected,

167   for samples collected in G1 prior to the onset of S phase, chromosomes migrated at their typical

168   positions in the CHEF gel (0 minute samples, Figure 1E). After release into S phase, both strains

169   began showing well-retention of chromosomes at the same time, indicating that the minimal

170   rDNA strain does not have a delayed start of chromosomal replication. However, the two strains

171   differed in their time of replication completion: Chromosomes IV (1531 kb) and VII (1090 kb)

172   were delayed by 10-15 minutes in the 35 rDNA *fob1Δ* strain (Figure 1F, S1F). The extent of

173   delay in replication completion appears to be proportional to chromosome length. We observed

174   a smaller delay in replication completion for Chromosome II (813 kb) and barely any delay for

175   chromosome VI (270 kb), the second smallest *S. cerevisiae* chromosome (Figure 1F, S1F-G).

176   We had difficulty quantifying Chromosome XII (containing the rDNA locus) for the wild type

177   rDNA strain: 56% of chromosome XII did not migrate into the gel, likely due to its large size

178   (Figure S1F, H). We instead quantified replication completion of intact rDNA arrays, using a

179   digest to separate the rDNA locus from its chromosomal context (Figure S1F). We found that a

180   higher fraction of the minimal rDNA array completed replication than the wild type rDNA array

181   (Figure 1F). We conclude that the minimal rDNA strain shows significant genome-wide delays

182   in completing chromosomal replication but fewer problems with completion of rDNA
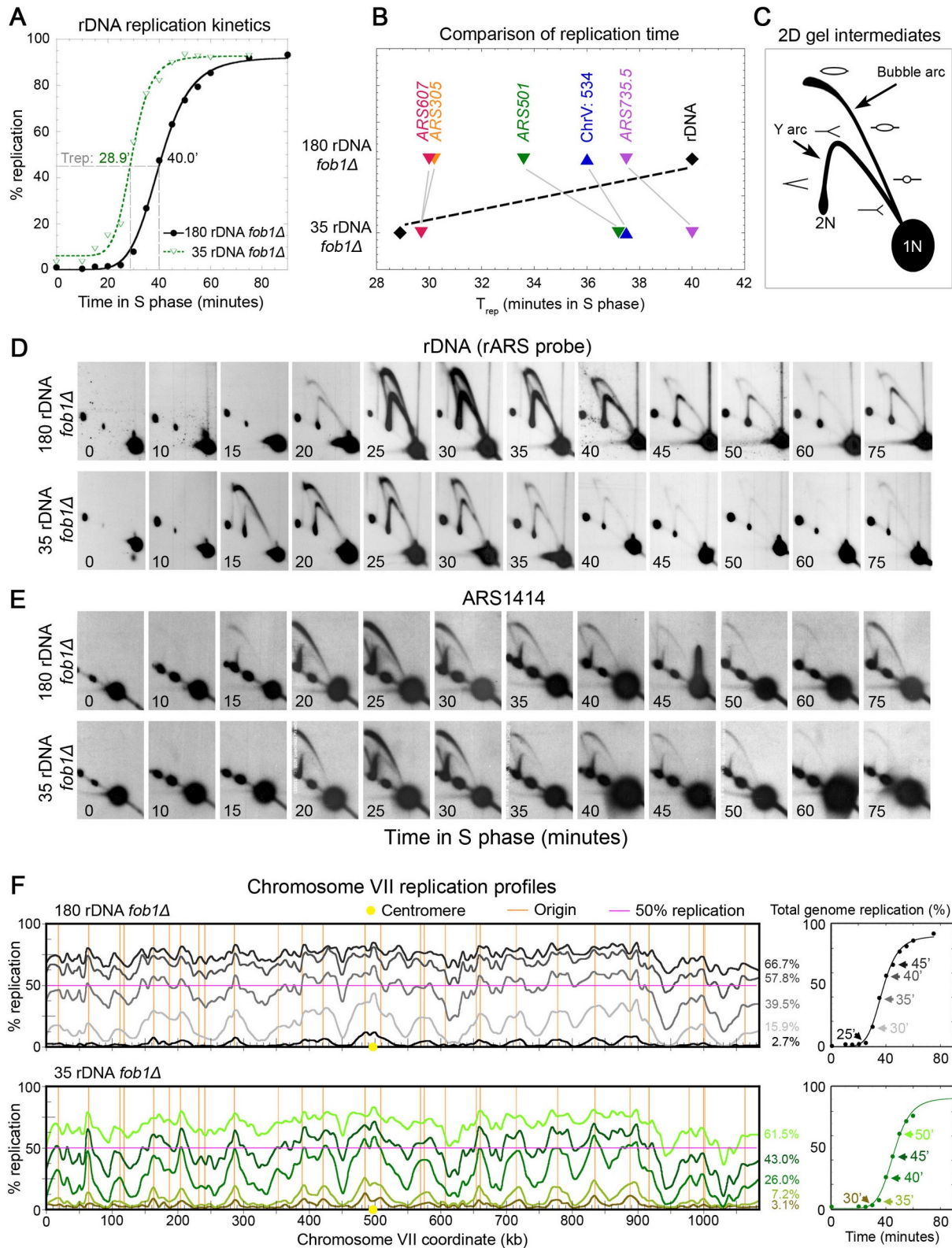
183   replication.

184

185   <u>Minimal rDNA strains advance rDNA replication and delay genome-wide replication</u>

186   To investigate the kinetics of genome-wide replication in strains with reduced rDNA

187   copy number, we performed density transfer experiments. Density transfer experiments exploit

188   the semi-conservative nature of DNA replication to distinguish newly replicated DNA from

189   unreplicated DNA at defined loci in the genome. Cells are grown in isotopically dense

190   ("heavy") medium, synchronized, and released into isotopically normal ("light") medium such

191   that the newly replicated DNA forms a "heavy/light" hybrid molecule. Hybrid replicated DNA

192   can be resolved from unreplicated dense DNA by cesium chloride gradient fractionation and

193   analyzed using quantitative Southern blotting and microarrays (Alvino et al., 2007; Raghuraman

194   et al., 2001). Although this method cannot distinguish active origin firing from passive DNA

195   replication, it allows us to identify replication differences across the genome. We collected

196   samples across an S phase and assessed replication kinetics both on an individual locus level and

197   on a genome-wide scale, confirming with flow cytometry that the minimal and wild type rDNA

198   strains showed similar G1 arrest and progression through S phase (Figure S2C).

199   We initially focused on the rDNA locus, which is late-replicating in *S. cerevisiae* and

200   several metazoan eukaryotic species (Coffman et al., 2005; Concia et al., 2018; Foss et al., 2017;

201   Labit et al., 2008; Schübeler et al., 2002). We calculated rDNA T_{rep}, the time at which half-

202   maximal replication was achieved, for each strain. While the rDNA locus was indeed late-

203   replicating in the wild type strain (T_{rep} =40.0'), the minimal rDNA array replicated earlier with a

204   T_{rep} of 28.9' (Figure 2A-B, S3A). In fact, the minimal rDNA locus was one of the earliest loci to

205   replicate rather than one of the latest (Figure 2B). The minimal rDNA[RM] array showed a similar

206   advancement of replication time (Figure S3B), indicating that minimal rDNA arrays replicate

207   early regardless of the rARS allele.

208   Because this drastic shift of rDNA replication timing from late to early might affect the

209   order in which replication factors are recruited to other genomic origins, we compared the

8

Figure 2: A minimal rDNA array replicates early and delays genome replication.

211 **Figure 2: A minimal rDNA array replicates early and delays genome replication.**

212 We calculated rDNA T_{rep}, the time at which half-maximal replication was achieved, for several loci. (A)
213 The minimal rDNA array replicates 11 minutes earlier than the 180-copy rDNA array. Replication kinetic
214 curves were generated from density transfer slot blot analysis. (B) Index of T_{rep} for different replication
215 origins and genomic region Chr. V: 534. (C) Diagram of a 2D gel showing locations of actively
216 replicating bubble or passively replicating Y intermediates. (D,E) 2D gel analysis of the rDNA origin of
217 replication (rARS) and *ARS1414* throughout S phase. (F) Replicating DNA from multiple density
218 transfer samples representing different time points were hybridized to microarrays and used to generate
219 genome-wide replication profiles. Chromosome VII replication profiles across S phase for the 180 rDNA
220 *fob1Δ* strain (top) and the 35 rDNA *fob1Δ* strain (bottom). Total genomic replication levels and time
221 interval are indicated on the right. Locations of centromere and origins of replication are noted by yellow
222 circles or orange lines. 50% replication threshold is denoted by pink horizontal line.

223 _____

224 replication kinetics for several other genomic loci (Figure 2B, S3C-D, Table S2). *ARS305* and

225 *ARS607*, two of the earliest and most efficient replication origins in *S. cerevisiae* (Friedman et

226 al., 1997; Hoang et al., 2007), did not differ greatly in timing between the minimal and wild type

227 rDNA strains. However, the late-replicating loci *ARS501* (also called *ARS522*), *ARS735.5*, and

228 ChrV:534000 without an origin (Ferguson and Fangman, 1992) were delayed in the minimal

229 rDNA strain, while their relative replication order was maintained.

231 <u>Altered replication timing is due to altered time of origin initiation</u>

232 The observed shifts of replication timing could be the result of changes to the time of

233 origin activation and/or efficiency. Although the rDNA kinetic curves (Figure 2A) suggested

234 that the minimal rDNA array began replicating earlier than the wild type array, we wanted to

235 directly examine replication initiation using 2D gel electrophoresis of synchronized cells

236 sampled across S phase. If the time of replication initiation was altered, we should observe

237 differences in when the replication "bubble" arc becomes visible among our strains (Figure 2C).

238 Strong rDNA origin (rARS) initiation in the minimal rDNA locus began robustly at 15 minutes

239 into S phase, whereas the wild type rDNA locus initiated replication later (at 20 minutes) (Figure

240 2D). These results confirm that early rDNA origin initiation is responsible for the earlier

241 replication of the minimal rDNA locus seen by density transfer.

242 The altered replication timing of other genomic loci was also confirmed by 2D gels. In

243 the minimal rDNA strain, we observed ~5-minute delays in replication initiation at late origins

10

244   such as *ARS1414* and *ARS735.5* (Figure 2E, S3E), with no apparent change in cumulative origin

245   use. We found no difference in initiation timing at the early, efficient *ARS305* (Figure S3F),

246   which reflects the density transfer data and is consistent with both the minimal rDNA and wild

247   type strains entering S phase at the same time. We conclude that the changes to replication

248   timing in the minimal rDNA strain are due to altered time of replication initiation at the rDNA

249   and at late non-rDNA origins of replication.

250

251   <u>Delayed replication progression is seen genome-wide in the minimal rDNA strains</u>

252   Since individual loci exhibited altered replication timing, we wanted to examine the

253   effects genome-wide in strains with early-replicating minimal rDNA arrays. We hybridized the

254   fractionated density transfer samples to microarrays and plotted percent replication against

255   chromosomal coordinates; these plots create chromosomal profiles that describe the landscape of

256   replication over time (Alvino et al., 2007; Raghuraman et al., 2001). We picked the earliest S

257   phase sample in which replication was detected and the three subsequent 5-minute intervals. In

258   the earliest sample with detectable hybrid density DNA at replication origins, we found only

259   subtle differences between the replication profiles of the minimal rDNA strain and that of the

260   wild type strain. (3.1% vs. 2.7% genome replicated, Figure 2F, S4, S5A-B). However, at the

261   next 5 minute interval, the minimal rDNA strain showed lower levels of replication completion

262   (7.2% genome replicated) compared to the wild type strain (15.9%) (Figure S5A). This trend

263   continued for the subsequent intervals, consistent with slower advancement of replication across

264   the genome for the minimal rDNA strain. We did not identify any specific genomic regions that

265   were preferentially altered in their replication profile; chromosome-wide replication profiles

266   from the minimal rDNA strain and wild type rDNA strain are superimposable when they achieve

267   similar levels of genome replication (Figure S5B). These data, together with the single locus

268   data, demonstrate that the minimal rDNA strain exhibits genome-wide replication delay without

269   region-specific effects.

270

271

11

272
273
274
275
276
277
278
279
280
281
282
283

284

285

286

287
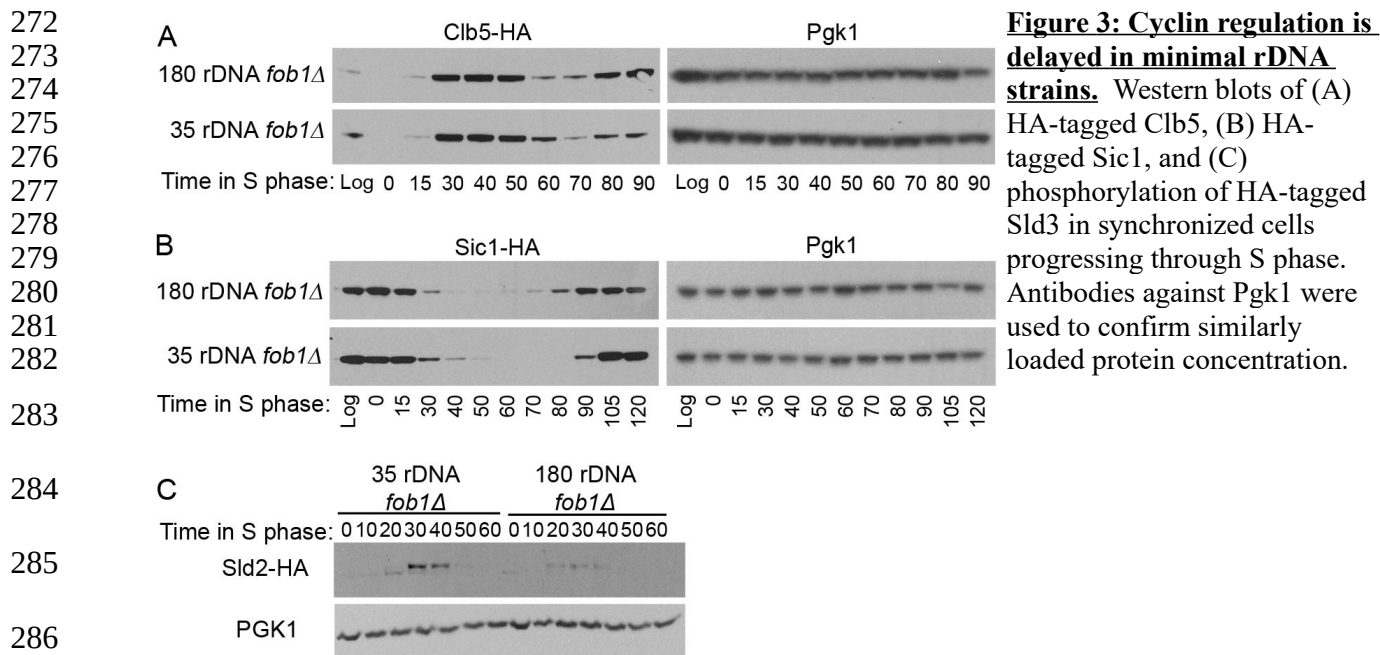
Figure 3: Cyclin regulation is delayed in minimal rDNA strains. Western blots of (A) HA-tagged Clb5, (B) HA-tagged Sic1, and (C) phosphorylation of HA-tagged Sld3 in synchronized cells progressing through S phase. Antibodies against Pgk1 were used to confirm similarly loaded protein concentration.

288   Cyclin regulation reflects DNA replication delays in cells with minimal rDNA

289   Delayed completion of genome replication should manifest as delayed appearance of cell

290   cycle landmarks. Such landmarks include the degradation of the CDK activator Clb5p (Schwob

291   and Nasmyth, 1993), the phosphorylation of limiting initiation factor Sld2p (Bloom and Cross,

292   2007; Lynch et al., 2019; Masumoto et al., 2002), and the reinstatement of the CDK inhibitor

293   Sic1p (Barberis et al., 2012; Khmelinskii et al., 2007; Schwob et al., 1994; Verma et al., 1997).

294   We separately tagged Clb5p, Sld2p, and Sic1p at their endogenous loci using a 3HA tag

295   (Longtine et al., 1998) in both the minimal rDNA and wild type rDNA strains. We then

296   collected synchronized samples for each strain throughout S phase for analysis via flow

297   cytometry and western blotting. The tagged minimal rDNA and wild type rDNA strains showed

298   similar S phase progression (Figure S2E). However, for cyclin signaling, the minimal rDNA

299   strain showed ~10-minute delays in the degradation of Clb5p-HA, the phosphorylation of Sld2p-

300   HA, and the degradation and reappearance of Sic1p-HA (Figure S3A-C). These delays in cyclin

301   signaling in the minimal rDNA strain match the strain's delayed genome-wide replication.

302

12

303   <u>How many rDNA origins in the minimal rDNA array initiate replication during early S phase?</u>

304   Approximately one in five of the rDNA origins is thought to serve as a replication

305   initiation site in cells with wild type rDNA (Brewer and Fangman, 1988; Linskens and

306   Huberman, 1988). By this estimate, a strain with 180 rDNA copies would have ~36 active

307   origins in the rDNA locus—close to the maximum number of possible rDNA origin initiations in

308   the minimal rDNA strains. We wondered how many rDNA origins fire in early S phase in the

309   minimal rDNA strain and if increased early rDNA firing would suffice to alter replication timing

310   genome-wide.

311   Digestion of replicating rDNA by the restriction enzyme NheI generates a variety of

312   distinct molecular intermediates/structures such as "bubbles" from active initiation, passively

313   replicated "Y" fragments, and "X" fragments produced by converging replication forks (Figure

314   4A), all of which can be resolved by 2D gel electrophoresis and Southern blotting (Figure 4B)

315   (Brewer and Fangman, 1988, 1987). However, accurate quantification of early rDNA initiation

316   requires the presence of the ribonucleotide reductase inhibitor hydroxyurea (HU) to slow down

317   fast-moving replication forks; these forks in *S. cerevisiae* travel at a rate of 1.5 kb per minute at

318   30ºC (Bell and Labib, 2016). Replication forks initiated at an rDNA origin will travel off the 4.7

319   kb origin-containing fragment (Figure 4A) in under 2 minutes and may fuse with oncoming

320   rDNA forks in ~3 minutes. We therefore released G1-synchronized cultures into S phase in the

321   presence of HU, which allowed us to capture more replication intermediates and limit initiation

322   events to early S phase (Alvino et al., 2007; Feng et al., 2006). In addition to the 4.7 kb rARS

323   fragment from every rDNA repeat, the NheI digest also generates a 24.4 kb single-copy rARS

324   fragment at the telomere proximal end of the rDNA array (Figure 4A-B). We used this single-

325   copy rDNA fragment for normalization, allowing us to generate a "per cell" estimate of active

326   rARS initiation in early S phase.

327   Compared to the wild type rDNA strain, the minimal rDNA strain showed a far stronger

328   rDNA bubble arc signal, which represents active replication initiations during S phase in HU

329   (Figure 4C, S5C). At the 30 minute time point, we estimate that the minimal rDNA strain had

330   9.1 rDNA initiations per cell whereas the wild type rDNA strain had less than one (Figure 4D).

331   This quantification is likely an underestimate due to the movement of replication off the
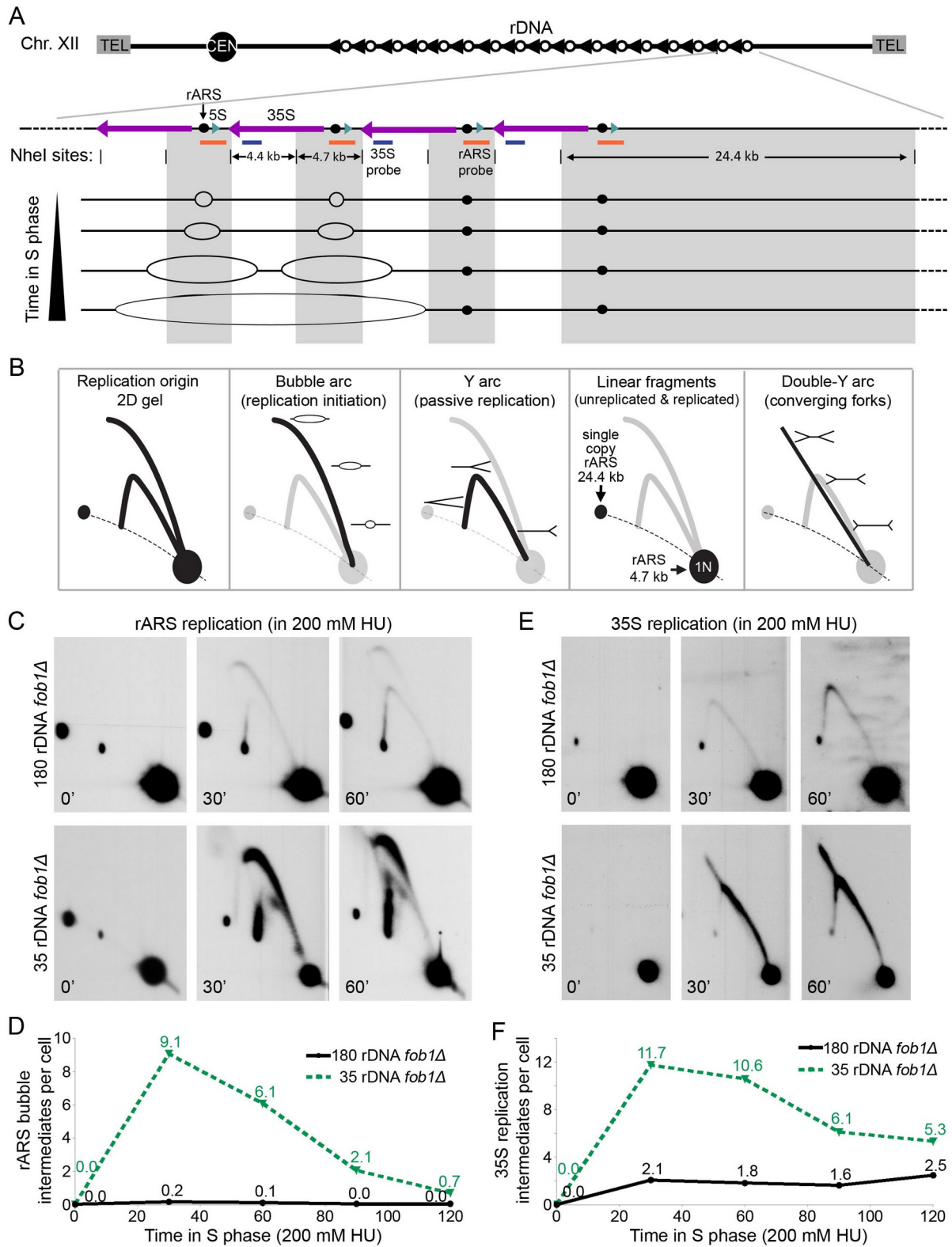
13

Figure 4: rDNA copy number reduction drives a 10-fold increase in rDNA replication initiation during early S phase.

14

334 **Figure 4: rDNA copy number reduction drives a 10-fold increase in rDNA replication initiation**
335 **during early S phase.** (A) Schematic of rDNA locus organization, relevant NheI-digest fragments,
336 Southern blot probe locations, and replication intermediates predicted throughout S phase. The 24.4 kb
337 fragment on the telomere proximal edge of the rDNA array serves as an internal reference for
338 quantification as it is present in a single copy per cell and hybridizes to the rARS probe. (B)
339 Representation of different replication intermediates on a 2D gel. (C,E) Timed 2D gels of cells released
340 into S phase in the presence of 200 mM HU. 2D gels were probed with both (C) the rARS probe
341 fragment and then (E) the 35S probe. Converging replication fork intermediates indicate initiation from
342 adjacent rDNA repeats and are seen in the strain with 35 rDNA copies but not the strain with 180 rDNA
343 copies. (D) Replication bubbles created by rARS initiations were quantified and normalized to the signal
344 in the single copy 24.4 kb linear spot. (F) Estimation of replication fork intermediates present in the
345 4.4kb NheI fragment without the rARS. Total replication fork signal was normalized to the 4.4 kb 1N
346 spot and adjusted for rDNA copy number.

347 _____

348 rARS-containing fragment (Figure 4A). Passively replicating Y-arc and convergent double-Y

349 intermediates (Figure 4B) seen in the adjacent non-origin 35S fragment (Figure 4E, S5D)

350 represent replication forks that have traveled from a neighboring rDNA origin. Quantification of

351 these Y and double-Y fragments relative to the linear 1N spot (Figure 4B) indicate that the wild

352 type rDNA array had an additional 2 initiation events per cell while the minimal rDNA array had

353 an additional 11 (Figure 4F). Combining active and passive replication values, we estimate that

354 the wild type strain contains 2 active rDNA origins in early S phase while the minimal rDNA

355 strain contains 20. Since the earliest replicating origin subset across the *S. cerevisiae* genome is

356 only 60 origins in a population of cells (Alvino et al., 2007; Yabuki et al., 2002), 18 additional

357 early-replicating rDNA origins in a single cell could easily generate significant competition for

358 limiting replication factors or nucleotides in early S phase (Mantiero et al., 2011; Shyian et al.,

359 2016) and cause the observed genome replication delays.

360

361 The increased DNA damage sensitivity in strains with reduced rDNA arises from a synthetic

362 interaction with *fob1Δ*

363   The genome replication delays in the minimal rDNA strain might contribute to the

364 strain's increased sensitivity to DNA damage; however, a previous study reported that the

365 additional, untranscribed rDNA copies protect cells from DNA damage by facilitating

366 recombinational repair (Ide 2010). We sought to disentangle the effects of early rDNA

15

367 replication and DNA repair on DNA damage sensitivity in the minimal rDNA strain by

368 considering two other mutants that replicate rDNA early: *rif1Δ* and *sir2Δ* (Figure 5).

369 Rif1p inhibits local replication initiation by recruiting protein phosphatase 1 (PP1,

370 Glc7p), which prevents the premature activation of the replication helicase subunit Mcm4p

371 (Davé et al., 2014, p. 1; Hiraga et al., 2014; Mattarocci et al., 2014). Because Rif1p binds at the

372 rARS (Hafner et al., 2018; Shyian et al., 2016), wild type rDNA arrays replicate early in Rif1p's

373 absence. Sir2p is a histone deacetylase responsible for silencing rDNA repeats. Without Sir2p,

374 reduced nucleosome occupancy and increased transcription at active rDNA repeats facilitate the

375 translocation of MCM helicases away from repressive chromatin environments (Foss et al.,

376 2019), likely generated by rARS-bound Rif1p. These unregulated MCM helicases drive early

377 replication initiation at the wild type-length rDNA arrays in *sir2Δ* mutants (Foss et al., 2017;

378 Saka et al., 2013; Yoshida et al., 2014). The minimal rDNA strain shares a critical feature with a

379 *sir2Δ* mutant: its rDNA array is also euchromatic and highly transcribed (French et al., 2003; Ide

380 et al., 2010), likely allowing loaded MCM helicases to translocate away from the rARS-bound

381 Rif1p.

382 Although the rDNA shifts to early replication in all three backgrounds – minimal rDNA,

383 *sir2Δ*, and *rif1Δ* – *sir2Δ* mutants did not show increased DNA damage (Figure 6B). This finding

384 seemed to exclude genome replication defects as a sole source of DNA damage sensitivity

385 because these defects were reported to be more severe in *sir2Δ* mutants than in strains with

386 reduced rDNA arrays (Foss et al., 2017; Yoshida et al., 2014). We first confirmed that loss of

387 *SIR2* results in early replicating rDNA (Figure 6C), although we observed no obvious increase in

388 cumulative rDNA origin initiation across S phase (Figure 6D). Second, as a proxy for plasmid

389 maintenance, we examined abundance of the 2 micron plasmid, whose numbers decrease in the

390 presence of replication defects (Maiti and Sinha, 1992; Storici et al., 1995). Both strains with

391 early replicating rDNA (*sir2Δ* and minimal rDNA) showed reduced 2 micron plasmid

392 abundance, to approximately 50% of the levels in wild type control strains (Figure 6E).

393 Because Sir2p plays a role in restricting genome-wide DNA replication (Hoggard et al.,

394 2020, 2018), we wondered if deletion of *SIR2* could rescue the minimal rDNA strain's sensitivity

395 to DNA damage and replication stress. We therefore examined MMS sensitivity upon *sir2Δ*
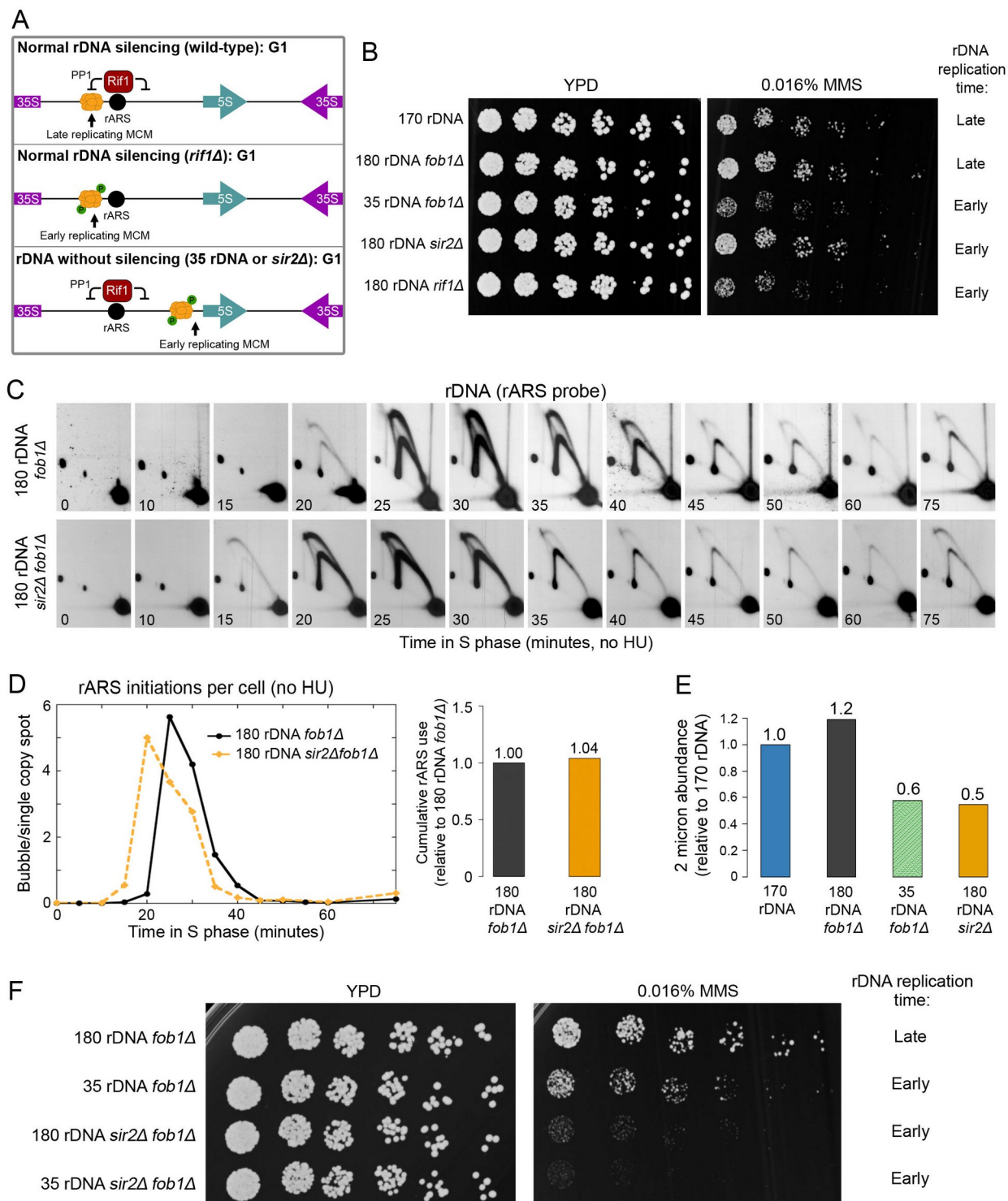
16

Figure 5: Sensitivity to MMS is due to a synthetic interaction between Fob1p and early rDNA replication.

398 **Figure 5: Sensitivity to MMS is due to a synthetic interaction between Fob1p and early rDNA**
399 **replication.** (A) Proposed mechanisms leading to early replicating rDNA. (B) The 35 rDNA *fob1Δ* strain
400 displays increased sensitivity to 0.016% MMS whereas the *sir2Δ* strain and *fob1Δ* strain show wild type
401 sensitivity. (C) Timed 2D gels of rDNA replication initiation in a 170 rDNA *sir2Δ fob1Δ* strain. (D)
402 Quantification of rDNA initiation signal per cell (relative to the 24.4 kb single copy rDNA spot) over the
403 course of S phase for 180 rDNA *fob1Δ,* 35 rDNA *fob1Δ*, and 180 rDNA *sir2Δ fob1Δ* strains. (E)
404 Abundance of the 2 micron plasmid, a parasitic element partially dependent on the *S. cerevisiae*
405 replication machinery, was assessed in logarithmically growing cells using quantitative Southern blotting
406 and normalized to a single copy genomic probe (ChrXV:810). (F) Deletion of *FOB1* increases MMS
407 sensitivity of strains with early replicating rDNA.

408 _____

409   deletion in the minimal rDNA strain and the wild type rDNA strain. To our surprise, deletion of

410 *SIR2* in a *fob1Δ* background led to increased MMS sensitivity regardless of rDNA copy number

411 (Figure 6F). This *fob1Δ* -dependent MMS sensitivity was reproducible among multiple strain

412 isolates, each of which was assessed for rDNA copy number (Figure S6A-B), confirming a

413 synthetic defect in DNA damage sensitivity between *fob1Δ* and *sir2Δ*.

414   Although the rDNA shifts to early replication in all three backgrounds – minimal rDNA,

415 *sir2Δ*, and *rif1Δ* – *sir2Δ* mutants did not show increased DNA damage (Figure 5B). This finding

416 seemed to exclude genome replication defects as a source of DNA damage sensitivity because

417 these defects were reported to be more severe in *sir2Δ* mutants than in strains with reduced

418 rDNA arrays (Foss et al., 2017; Yoshida et al., 2014). We first confirmed that loss of *SIR2*

419 results in early replicating rDNA (Figure 5C), although we observed no obvious increase in

420 cumulative rDNA origin initiation across S phase (Figure 5D). Second, as a proxy for plasmid

421 maintenance, we examined abundance of the 2 micron plasmid, whose numbers decrease in the

422 presence of replication defects (Maiti and Sinha, 1992; Storici et al., 1995). Both strains with

423 early replicating rDNA (*sir2Δ* and minimal rDNA) showed reduced 2 micron plasmid

424 abundance, to approximately 50% of the levels in wild type control strains (Figure 5E).

425   Because Sir2p plays a role in restricting genome-wide DNA replication (Hoggard et al.,

426 2020, 2018), we wondered if deletion of *SIR2* could rescue the minimal rDNA strain's sensitivity

427 to DNA damage and replication stress. We therefore examined MMS sensitivity upon *sir2Δ*

428 deletion in the minimal rDNA strain and the wild type rDNA strain. To our surprise, deletion of

429 *SIR2* in a *fob1Δ* background led to increased MMS sensitivity regardless of rDNA copy number

430 (Figure 5F). This *fob1Δ* -dependent MMS sensitivity was reproducible among multiple strain

431   isolates, each of which was assessed for rDNA copy number (Figure S6A-B), confirming a

432   synthetic defect in DNA damage sensitivity between *fob1Δ* and *sir2Δ*.

433   We considered that *fob1Δ* might drive sensitivity of strains with early rDNA replication

434   to DNA damage/replication stress. The *fob1Δ* mutation is required to prevent expansion of

435   reduced rDNA arrays (Kobayashi et al., 1998), making it challenging to assess the consequences

436   of the minimal rDNA array in a wild type background. However, we hoped that the rDNA

437   expansion after *FOB1* restoration might be slow enough to capture and assess DNA damage

438   sensitivity of a short rDNA array. To this end, we examined spores from a cross of the minimal

439   rDNA strain (35 rDNA copies; *fob1Δ*) strain with a *MATα* 150 rDNA *FOB1* strain. Each spore

440   was allowed to form a colony, which was immediately inoculated into culture, and both rDNA

441   copy number and MMS sensitivity were assessed from the same culture. The isolated *FOB1* and

442   *fob1Δ* cells with short rDNA had approximately 55 rDNA copies when plated on MMS (Figure

443   S6C). As suitable controls, we employed the previously engineered *fob1Δ* strains with 55 and 80

444   rDNA copies, with the former exhibiting greater sensitivity to MMS than the latter. The *FOB1*

445   cells with 55 rDNA copies were more resistant to MMS than *fob1Δ* cells with 55 rDNA copies or

446   minimal rDNA; there was no discernible difference between *FOB1* and *fob1Δ* cells with 150

447   rDNA copies (Figure S6D). Thus, it is the loss of *FOB1* in combination with rDNA reduction

448   and/or early rDNA replication that causes sensitivity to DNA damage. We therefore propose that

449   the presence of Fob1p itself plays a significant role in the mitigation of early rDNA replication

450   effects, outside of the genome replication delays we observed and the previously reported DNA

451   damage sensitivity (Ide et al., 2010).

452

453   <u>The mitotic exit regulator Cdc14 is mislocalized in the minimal rDNA strain</u>

454   The replication fork-block protein Fob1p has other roles in addition to its eponymous

455   <u>FO</u>rk-<u>B</u>locking activity (Krawczyk et al., 2014; Salim et al., 2021; Ward et al., 2000), including

456   sequestration of the mitotic-exit phosphatase Cdc14p (Huang and Moazed, 2003; Stegmeier et

457   al., 2004). We focused on Cdc14p sequestration since delayed genome replication could alter

458   mitotic exit. Cdc14p is recruited to two regions of the rDNA: at the Replication Fork Barrier

459   (RFB) where it is bound to Fob1p and upstream of the 35S transcription start site where it is

460   bound by a yet unidentified factor (Figure S7A; Huang et al., 2006; Huang and Moazed, 2003;

461   Stegmeier et al., 2004). Cdc14p is sequestered in the nucleolus until its release to the nucleus

462   during early anaphase and to the cytoplasm during late anaphase and mitotic exit (Mohl et al.,

463   2009; Shou et al., 1999; Stegmeier et al., 2004; Visintin et al., 1999).

464   We were curious to determine whether Cdc14p localization would be altered by rDNA

465   copy number reduction in a *fob1Δ* mutant background. We examined localization of Cdc14p-

466   GFP in comparison to DAPI-stained nuclei in both the minimal rDNA and wild type rDNA

467   strains arrested in G1. Almost 90% of wild type rDNA cells showed Cdc14p-GFP normally

468   sequestered to the nucleolus, which excludes DAPI (Figure 6A-B); the remaining cells with

469   Cdc14p-GFP overlapping the DAPI-stained nucleus are likely a consequence of their nucleoli

470   being above or below the nucleus during microscopy. In the minimal rDNA strain, a mere

471   32.2% of G1 cells showed nucleolar Cdc14p-GFP, with 67.8% of cells showing diffuse nuclear

472   Cdc14p-GFP.

473   This aberrant Cdc14p localization is not due to a loss of nucleolar integrity. We

474   examined nucleolar structure in our strains using a GFP fusion of Utp13p, a nucleolar protein

475   involved in ribosome biogenesis (Huh et al., 2003; Woolford and Baserga, 2013). Utp13p-GFP

476   localization was identical in both the minimal rDNA and the wild type rDNA strains (Figure 6B-

477   C), indicating that nucleolar structure was not altered, consistent with previous findings (Dauban

478   et al., 2019). The minimal rDNA strain's aberrant Cdc14p-GFP localization is consistent with a

479   mitotic exit defect that exacerbates effects from delayed genome replication.

480

481   <u>A redundant mitotic exit checkpoint in yeast?</u>

482   If Cdc14p is involved in coordinating genome replication and mitotic exit, we would

483   expect delayed anaphase entry to accommodate the genome replication defects in strains with

484   early rDNA replication. Given the substantial delays in DNA replication and cyclin signaling,

485   we anticipated late anaphase entry in all strains with early replicating rDNA: the 35 rDNA *fob1Δ*

486   strain, and the *sir2Δ* and *rif1Δ* single mutants. We examined DAPI-stained nuclear morphology

487   across S phase as a proxy for entry into anaphase ((Hartwell et al., 1974; Yellman and Roeder,
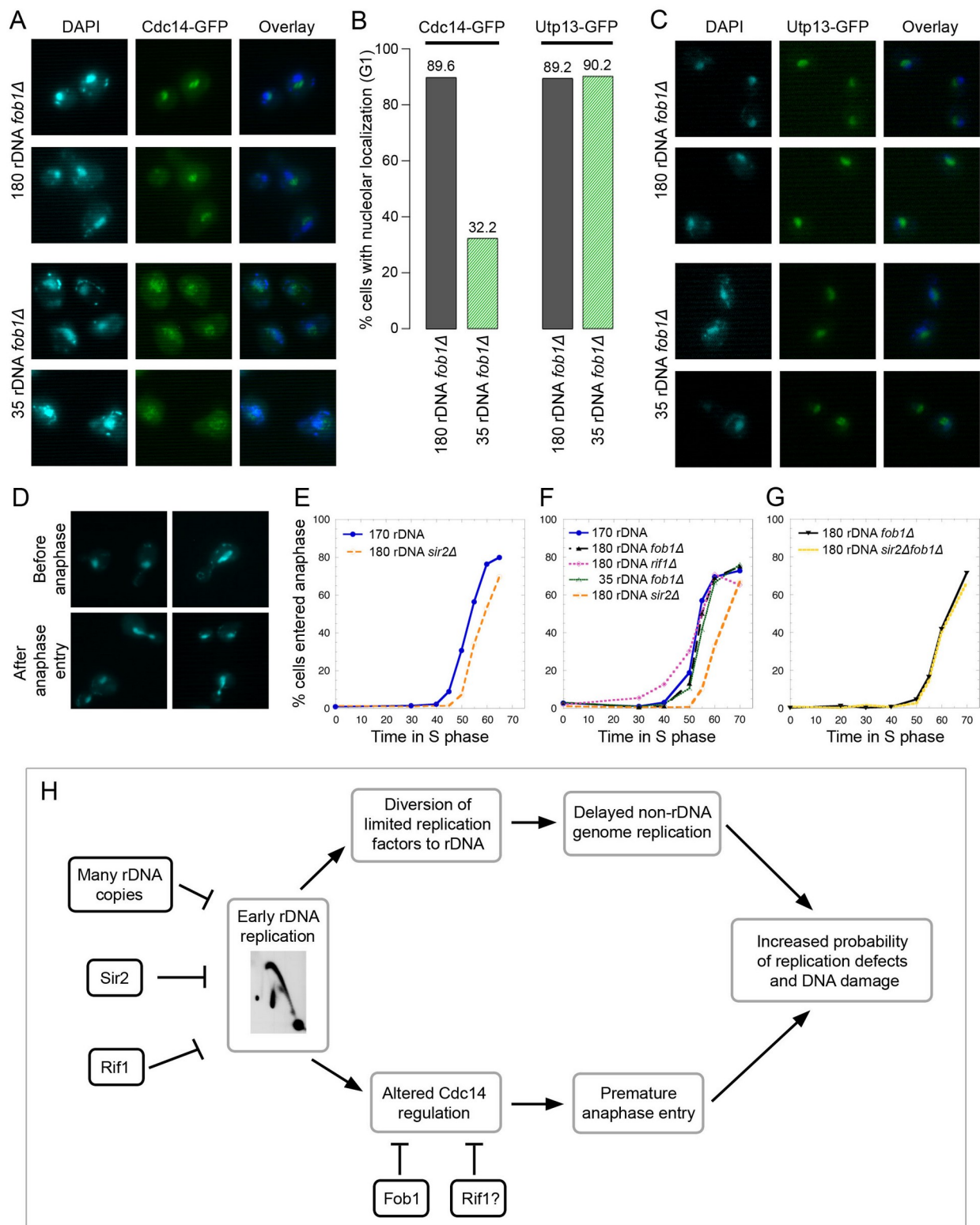
20

Figure 6: Minimal rDNA strains show poor nucleolar sequestration of Cdc14p and premature anaphase entry.

21

490 **Figure 6: Minimal rDNA strains show poor nucleolar sequestration of Cdc14p and premature**
491 **anaphase entry.** (A) C-terminally tagged Cdc14-GFP was visualized in 180 rDNA *fob1Δ* and 35 rDNA
492 *fob1Δ* cells. (B) Quantification of G1 cells with nucleolar localization of Cdc14-GFP or Utp13-GFP. (C)
493 Utp13-GFP, a nucleolar protein that is involved in rRNA processing, was used to ascertain nucleolar
494 structure (Woolford and Baserga 2013). Both 35 rDNA *fob1Δ* and 180 rDNA *fob1Δ* cells show normal
495 nucleolar structure. (D) Examples of DAPI-stained nuclei representing cells scored as either being
496 "before anaphase" or "after anaphase entry." (E-G) Quantification of percentage of cells that had entered
497 anaphase for each strain over time. (H) Proposed model regarding consequences of rDNA copy number
498 reduction and early rDNA replication.

499 _____

500 2015), Figure 6D). As anticipated, the *sir2Δ* mutant entered anaphase later than the wild type

501 (Figure 6E-F). However, both the minimal rDNA strain and the *rif1Δ* strain entered anaphase at

502 the same time or earlier than their wild type control strains, suggesting that these mutants have

503 lost the mechanism to delay anaphase in response to delayed genome replication (Figure 6F).

504 The link between genome replication status and anaphase entry appears to be partially dependent

505 on *FOB1*: no difference was observed in anaphase entry between *sir2Δ* and *SIR2* strains in the

506 absence of *FOB1* (Figure 6G). The observed disconnect between S phase completion and

507 anaphase entry mirrors our earlier results with the MMS sensitivity assay: the minimal rDNA,

508 *rif1Δ* and *sir2Δ fob1Δ* strains showed anaphase progression in spite of replication delays as well

509 as increased MMS sensitivity (Figure 5B, F). The *FOB1*-dependent coordination between

510 anaphase entry and genome replication completion suggests that Fob1p acts as a redundant,

511 yeast-specific checkpoint for S phase completion functioning in concert with Cdc14p

512 sequestration (Figure S7).

513

514 **DISCUSSION**:

515 Minimal rDNA arrays replicate early and delay genome replication

516 Here, we characterized the replication consequences of reducing the *S. cerevisiae* rDNA

517 locus from its wild type ~180 copies to a minimal array of 35 copies. We found altered

518 replication timing not just at the rDNA locus but also across the genome. The minimal rDNA

519 array replicates at the very earliest part of S-phase whereas the full-length rDNA is among the

520 latest replicating regions. This shift in replication timing is explained by the ~20 additional

22

521   rDNA initiations that occur in the minimal rDNA array in early S phase. We propose that these

522   additional early-replicating rDNA origins divert the limiting factors required to activate non-

523   rDNA origins, thereby creating delays in replication elsewhere in the genome. Our findings

524   contradict previous interpretations of similar data, whose authors concluded that rDNA copy

525   number reduction leads to replication defects only at the rDNA locus and not in the rest of the

526   genome (Ide et al., 2010). However, replication of other large chromosomes appears visibly

527   impaired in their manuscript (Ide et al. 2010, Figure 2D), consistent with our findings and

528   interpretation.

529   The dramatic shift of rDNA replication to the early part of S-phase in the minimal rDNA

530   strains comes at a price: impaired plasmid maintenance, heightened sensitivity to HU and MMS,

531   and delayed genome replication. It appears paradoxical that reducing rDNA copy number

532   generates replication stress given that the full-length wild type rDNA array is dramatically

533   shortened in many conditions of imposed replication stress, either in the presence of DNA

534   replication mutants or limiting conditions like HU (Ide et al., 2007; Lynch et al., 2019; Salim et

535   al., 2017; Sanchez et al., 2017). Indeed, rDNA copy number reduction has been proposed to be a

536   compensatory mechanism for replication stress (Ide et al., 2007; Kwan et al., 2013; Salim et al.,

537   2017). We argue that rDNA copy number reduction will affect genome replication only if the

538   rDNA replication timing is affected. This argument is supported by earlier studies describing a

539   mutant that induces replication stress and reduces rDNA copy number (Lynch et al., 2019). The

540   reduced rDNA array in this mutant remained late-replicating, possibly because its copy number

541   reduction was not severe enough to alter replication timing. Further work is necessary to

542   determine the copy number reduction leading to early rDNA replication and whether this shift in

543   replication time is gradual or precipitous.

544

545   <u>A synthetic interaction between early rDNA replication and *FOB1* explains sensitivity to DNA</u>

546   <u>damage in strains with reduced rDNA copy number</u>

547   Early replicating rDNA causes genome replication defects (this study, (Foss et al., 2017;

548   Ide et al., 2010; Shyian et al., 2016; Yoshida et al., 2014)), yet the increased DNA-damage

549   sensitivity in strains with early-replicating rDNA is not solely a response to delayed genome-

23

550   wide replication. As we show, *sir2Δ* single mutants have early replicating rDNA with wild type

551   copy number and suffer genome-wide replication defects (Foss et al., 2017) but this background

552   is not sensitive to DNA damage. Comparing the *sir2Δ fob1Δ* and *sir2Δ* strains*,* we identified a

553   synthetic interaction between *fob1Δ* and early rDNA replication, which results in increased

554   sensitivity to the DNA-alkylating agent MMS.

555   Previous studies proposed that reduced rDNA copy number sensitizes strains to DNA

556   damage because DNA repair is impaired in short arrays in which all copies are transcribed (Ide

557   et al., 2010). This interpretation was based on the observation that a deletion of the PolI-subunit

558   *RPA135*, and consequently cessation of endogenous rDNA transcription, erased the difference in

559   MMS sensitivity between a 20-copy rDNA strain and a strain purportedly carrying 110 copies.

560   However, deletions of rDNA transcription machinery, including *RPA135*, result in an 80%

561   reduction in rDNA copy number (Brewer et al., 1992; Kobayashi et al., 1998). Thus, the

562   similarity in MMS sensitivity between the two strains could simply stem from similarly low

563   rDNA copy number, which was not verified in the study (Ide et al., 2010).

564   Moreover, the MMS-sensitive phenotype of the *sir2Δ fob1Δ* strain, which contains over

565   150 rDNA copies, is inconsistent with the model proposed by Ide *et al.* This strain should have

566   sufficient DNA repair capacity because loss of *SIR2* only moderately increases the number of

567   accessible, presumably actively transcribed rDNA copies (*i.e.* 40% accessible vs 60% non-

568   accessible in wild type yeast; 50% accessible vs 50% non-accessible in *sir2Δ*, (Smith and Boeke,

569   1997)). However, in our hands, the *sir2Δ fob1Δ* strain shows possibly even greater MMS

570   sensitivity than the minimal rDNA *fob1Δ* strain (Figure 6E). Taken together, our results

571   demonstrate that the capacity for DNA damage repair provided by additional, silenced rDNA

572   copies does not explain the sensitivity of reduced rDNA strains to DNA damage.

573

574   The synthetic interaction between early rDNA replication and *FOB1* uncovers a putative cell

575   cycle checkpoint in yeast

24

576   Considering prior evidence and our findings, we propose a model explaining 1) how

577   rDNA replication might coordinate whole genome replication and anaphase entry and 2) how

578   Fob1p might function as a redundant checkpoint in Cdc14 sequestration and mitotic exit.

579   In a wild type yeast cell (Figure S7A), ~2000 Cdc14p molecules (Cherry et al., 2012; Ho

580   et al., 2018; Kulak et al., 2014) are sequestered at two sites within an rDNA repeat: at the

581   transcription start site (TSS) and the replication fork barrier (RFB) bound by Fob1p. Cdc14p

582   remains bound at all 180 rDNA repeats during G1 and early S phase. In late S phase, 36 rDNA

583   origins fire and replication forks begin to dislodge Cdc14p from the nearby TSS, but Cdc14p

584   remains bound to Fob1p at the 180 RFB sites. Fob1p, which enforces unidirectional replication

585   (Brewer and Fangman, 1988; Linskens and Huberman, 1988), acts as second, more stable tether

586   for Cdc14p because the RFB can only be replicated by an oncoming fork from an adjacent active

587   origin. Given that a 1 in 5 rDNA origins initiate in a wild type cell (Brewer and Fangman, 1988;

588   Linskens and Huberman, 1988), the nearest active origin is ~45 kb (5 rDNA arrays) away on

589   average, and it will take the replication machinery ~30 minutes to reach the stalled fork. Hence,

590   rDNA will complete replication 30 minutes after rDNA origins fire in S phase, consistent with

591   the rDNA locus as the very last region to complete replication. Thus, Cdc14p remains

592   sequestered in the very last region of the genome to replicate, to be fully dislodged by replication

593   at the very end of S phase. We posit that full replication of the rDNA signals the genome-wide

594   replication completion and enables subsequent anaphase entry through Cdc14p release.

595   In a *fob1Δ* mutant with wild type rDNA copy number (Figure S7B), Cdc14p is not bound

596   to the RFB, but remains associated with the rDNA TSS until rDNA replication completion in late

597   S/early anaphase (Stegmeier et al., 2004). The wild type-length rDNA is still replicated in late S

598   phase and the genome finishes replication by the time of complete Cdc14p release, maintaining

599   coordination of both replication processes. The *fob1Δ* strain retains wild type sensitivity to DNA

600   damage and replication stress agents.

601   In a *fob1Δ* mutant with minimal rDNA copy number (Figure S7C), Cdc14p nucleolar

602   localization is severely disrupted even prior to S phase. The 35 rDNA copies do not provide

603   enough binding sites for Cdc14p, in particular because Fob1p is missing at the RFB. The

604   minimal rDNA array replicates early, which dislodges Cdc14p fully in early to mid S phase.

605 Free, unsequestered Cdc14p l will induce anaphase entry while the genome has not yet

606 completed replication. This disconnect between completion of genome replication and anaphase

607 entry may lead to premature cell cycle progression without allowing sufficient time for DNA

608 repair, resulting in increased sensitivity to DNA damage and replication stress agents (Figure 2B,

609 6A).

610 In a *sir2Δ* mutant with wild type rDNA copy number (Figure S7D), the rDNA replicates

611 early while replication delays occur elsewhere. This strain shows wild type sensitivity to DNA

612 damage (MMS, Figure 6A). The presence of Fob1p promotes the retention of Cdc14p at the

613 RFB and also enforces slower, unidirectional rDNA replication. Although the rDNA array

614 replicates early, it would still take ~30 minutes for rDNA replication to be complete. During this

615 time, Cdc14p will remain bound to the RFB via Fob1p while the genome will complete

616 replication, apparently even with rDNA-induced delays. In this way, anaphase entry remains

617 coordinated with genome replication completion. Consistent with this interpretation, we

618 observed delayed anaphase in *sir2Δ* single mutant strains, which suggest anaphase entry remains

619 coordinated with genome replication.

620 In a *sir2Δ fob1Δ* mutant with wild type rDNA copy number (Figure S7E), Cdc14p is

621 sufficiently bound to the rDNA array in G1, but is missing at RFBs because of the absence of

622 Fob1p. Fob1p absence also leads to more rapid, bidirectional replication of the rDNA array,

623 which is completed in 15 minutes in this strain. This early and rapid replication of the rDNA

624 array will dislodge Cdc14p from the nucleolus while the rest of the genome is in the midst of

625 replicating. Therefore, the *sir2Δ fob1Δ* strain loses coordination between completion of genome

626 replication and anaphase entry, resulting in increased sensitivity to DNA damage (Figure 6E,

627 7G).

628 Taken together, the evolutionarily conserved excess of rDNA copies in concert with their

629 late replication act as checkpoint for whole genome replication via Cdc14p sequestration in the

630 nucleolus. Cdc14p sequestration redundantly requires the presence of the yeast-specific Fob1p

631 at RFBs.

632

633   <u>rDNA copy number and genome replication: implications for disease</u>

634   rDNA copy number can affect the essential processes of whole genome replication and

635   cell cycle progression, extending the phenotypic impact of this genomic element far beyond

636   ribosome biogenesis (Figure 7H). Although *S. cerevisiae* populations typically maintain strain-

637   specific rDNA copy number (Kwan et al., 2016), the repetitive nature of rDNA arrays can allow

638   for rare array contraction below the range of natural variation. Thus, rDNA copy number should

639   be taken into consideration as a background variable when interpreting the consequences of

640   other genetic variants. In fact, rDNA copy number changes are frequently observed after

641   standard *S. cerevisiae* genetic manipulation practices (Kwan et al., 2016).

642   For metazoans, rDNA copy number reduction may have implications for health

643   outcomes. A recent study reports that rDNA copy number reduction precedes pathogenesis in an

644   mTOR-activated cancer mouse model, suggesting that rDNA reductions may act as driver

645   mutations in certain cancers (Wang and Lemos, 2017; Xu et al., 2017). Hutchinson-Gilford

646   progeroid cell lines show bloated nucleoli (Buchwalter and Hetzer, 2017) and increased DNA

647   damage that appears late in S phase (Chojnowski et al., 2020), echoing phenotypes observed in

648   yeast strains with early replicating rDNA. Although the replication fork barrier protein Fob1p

649   itself is not conserved in metazoans, some Cdc14p homologs are known to localize to the

650   nucleolus (Berdougo et al., 2008; Kaiser et al., 2004; Manzano-López and Monje-Casas, 2020;

651   Saito et al., 2004; Wu et al., 2008). Cdc14p regulation in metazoans may be more sensitive to

652   early rDNA replication without the redundant Fob1p tether.

653

654   <u>How plausible is DNA replication as a gauge of whole genome replication status?</u>

655   While the nucleolus was originally deemed an oddly mundane location for such an

656   exciting molecule, Cdc14p sequestration in the nucleolus is now recognized as an important

657   hallmark of cell cycle regulation (Amon, 2008). We argue that this mundane organelle, and

658   Cdc14p's localization within in it, are ideal for cell cycle control. Every cell contains nucleoli,

659   membrane-free organelles that form around the rDNA arrays. Nucleoli and rDNA transcription

660   are highly responsive to cell and organismal physiology, including nutritional status, stress, and

27

661 aging. The rDNA is late-replicating and associated with Cdc14p whose release into the nucleus

662 coincides with anaphase entry (Figure 7H). The late replication of the rDNA locus may be

663 conserved across a wide variety of species in order to both mitigate replication competition and

664 coordinate replication status with cell cycle progression.

665

676

677 **Author contributions:**

678 Conceptualization, E.X.K., G.M.A., B.J.B., C.Q., and M.K.R; Methodology, E.X.K., G.M.A.,

679 B.J.B., and M.K.R.; Investigation, E.X.K., G.M.A., K.L.L., P.F.L., H.M.A., X.S.W., S.A.J.,

680 J.C.S., M.A.M., M.C., S.B.L., and M.N.; Resources, E.X.K., G.M.A., B.J.B., and M.K.R.;

681 Writing - Original Draft, E.X.K, G.M.A., B.J.B., C.Q., and M.K.R.; Writing - Review & Editing,

682 E.X.K., G.M.A., K.L.L., B.J.B., C.Q., and M.K.R.; Supervision: B.J.B., J.T.C., C.Q., and

683 M.K.R.; Funding Acquisition, B.J.B., M.K.R., and C.Q.

684

685 **Declaration of interests:**

686 The authors declare no competing interests.

687

688 **MATERIALS AND METHODS**:

689 Yeast strains, probe fragments, plasmids, and media:

690 Yeast strains used are listed in Supplementary Table 1. Yeast strains were grown, unless noted

691 otherwise, in synthetic complete media buffered with 1% succinic acid (per liter: 1.45g yeast

692 nitrogen base, 20 g glucose, 10 g succinic acid, 6 g NaOH, 5 g $(NH_4)_2SO_4$, 2.8 g amino acid

693 powder mix with pH adjusted to 5.8). In cases when YPD medium is used, per liter: 20 g bacto

694 peptone, 10 g yeast extract, and 20 g glucose.

695 Since we were concerned about possible *de novo* rDNA copy number changes over the

696 course of this study, we froze multiple samples from log-phase cultures that had been CHEF gel

697 verified (Figure 1B), and used these frozen stocks as inoculants for each experiment.

698

699 rDNA reduction:

700 S288c *fob1Δ* strains transformed with the pRDN1-Hyg plasmid, were first isolated by selection

701 for uracil prototrophy, then plated onto medium containing hygromycin B to select for rDNA

702 copy number reduction (Chernoff et al., 1994; Kobayashi et al., 2001; Kwan et al., 2013).

703 Individual colonies were picked for screening by CHEF gel electrophoresis to measure rDNA

704 copy number (Figure S1). We identified and isolated strains with 35, 45, and 55 copies of rDNA

705 and decided to focus on strains with 35 rDNA copies ("35 rDNA *fob1Δ*" and "35 rDNA[RM]

706 *fob1Δ*"), restoring endogenous *URA3* to facilitate downstream replication assays. Genetic

707 crosses were used generate prototrophic strains and GFP-tagged strains.

708

709 During the isolation of strains with reduced rDNA copy number by this pRDN1-HYG plasmid

710 method, we noticed that 20-25% of the isolates with rDNA reductions had either diploidized or

711 tetraploidized (Figure S1), something we had not previously observed when constructing strains

712 by transformation. Subsequently, we verified ploidy of each strain for each experiment by flow

713 cytometry and used only confirmed haploid strains for each experiment. This frequent increase

714 in ploidy may be related to rDNA reduction by this pRDN1-Hyg method. While interesting, we

29

715   have not identified the biological mechanism involved and strongly suggest verifying ploidy

716   when this rDNA reduction method is employed in the future.

717

718   <u>Preparation of DNA in agarose plugs:</u>

719   DNA was isolated in agarose plugs according to previously published protocols (Tsuchiyama et

720   al., 2013). Each 90 µL plug contained either ~10^8 stationary phase cells for CHEF gels, ~5×10^7

721   log phase cells for rDNA 2D gels, or ~10^8 log phase cells for single-copy origin 2D gels.

722   Collected cells were washed with 50 mM EDTA, resuspended in 90 µL 0.5% SeaPlaque GTG

723   agarose in 50 mM EDTA, and transferred into plug molds. Once solidified, plugs were

724   incubated in 1 mL spheroplasting solution (1 M sorbitol, 20 mM EDTA, 10 mM Tris-HCl pH7.5,

725   14 mM β-mercaptoethanol, 0.5 mg/mL Zymolyase-20T (Amsbio)) for 2-5 hours at 37ºC. Plugs

726   were washed once with LDS (1 % lithium dodecyl sulfate, 100 mM EDTA, 10 mM Tris–HCl pH

727   8.0) and incubated overnight at 37ºC in LDS overnight with gentle shaking. Plugs were then

728   washed 3 x 30 minutes in 0.2X NDS (1X NDS pH 9.5: 0.5 M EDTA, 10 mM Tris base, 1%

729   Sarkosyl) and 5 x 30 minutes in TE pH 8.0. Processed plugs were stored at 4ºC in TE pH 8.0

730   until use.

731

732   <u>CHEF gel analysis:</u>

733   We used contour-clamped homogeneous electric field (CHEF) gel electrophoresis to resolve

734   intact *S. cerevisiae* chromosomes. A slice of each genomic DNA agarose plug was embedded in

735   a 0.8% agarose gel (0.5X TBE) and each gel contained one wildtype sample as reference. For

736   most CHEF gels, we ran the samples in 2.3L of 0.5X TBE using a Bio-Rad CHEF-DRII

737   electrophoresis cell at 100V for 66 hours (switch time = 300 to 900 seconds). The gels were

738   then stained with ethidium bromide to visualize all chromosomes, including the rDNA-

739   containing chromosome XII. To examine the size of the excised rDNA array, genomic DNA

740   samples in plugs were digested with BamHI or FspI and then run on a 0.8% CHEF gel at 165 V

741   for 64 hours (switch time = 47 to 170 seconds). Chromosome XII size and rDNA copy number

742 were further examined via Southern blotting. For size comparison, known standards (*H. wingei*

743 and/or Yeast Ladder from New England BioLabs) were included in each CHEF gel run.

744

745 <u>Sample collection for chromosome replication completion assay:</u>

746 Cells were grown to mid-logarithmic phase (2.5×10^6 cell/mL) , arrested in G1 with 3 μM α-

747 factor, and released into S phase (by the addition of 0.15 mg/mL Pronase (EMD Millipore)) in

748 the presence of 0.008% MMS. Samples were collected every 20 minutes for CHEF gel

749 electrophoresis and prepared as described above in agarose plugs for CHEF gel electrophoresis.

750 The same Southern blot membrane was probed for all measured chromosomes except for the

751 FspI-excised rDNA.

752

753 <u>Southern blotting:</u>

754 Each gel was transferred to a GeneScreen Hybridization membrane using standard Southern

755 blotting protocols (Tsuchiyama et al., 2013) We then hybridized each sequence of interest using

756 a ^{32}P-labeled probe. The blots were exposed to X-ray film and to Bio-Rad Molecular Imaging

757 FX phosphor screens for visualization and quantification of signal intensity. Phosphor screens

758 were scanned using a Bio-Rad Personal Molecular Imaging scanner and analyzed using Bio-

759 Rad's Quantity One software. Southern blots were often stripped and re-probed with a different

760 sequence of interest (CHEF gel blots, 2D gel blots, density transfer blots). To strip a Southern

761 blot, blots were subjected to two washes of 20 minutes each in 500 mL stripping buffer (0.1%

762 SSC; 1% SDS) that had been heated to 100°C. Blot stripping efficacy was gauged by exposure

763 and quantification of phosphor screens before the next probe hybridization.

764

765 <u>rRNA quantification:</u>

766 rRNA quantification was performed as described (Sanchez et al., 2017). Asynchronous

767 logarithmic phase cells were collected and nucleic acids (RNA and DNA) were isolated using a

768 "Smash & Grab" phenol:chloroform extraction protocol (Radford, 1991). The RNA northern

31

769   blot was hybridized to a ^{32}P-labeled probe for the 25S rRNA sequence. To assess loading

770   normalization, the DNA Southern blot portion was hybridized to a ^{32}P-labeled probe for *ACT1*, a

771   single copy gene. The rRNA and *ACT1* blots were separately exposed to S Bio-Rad phosphor

772   screens and *25S* rRNA and *ACT1* DNA intensity was quantified using a Bio-Rad Personal

773   Molecular Imager and Bio-Rad Quantity One software.

774

Density transfer:

776   The density transfer protocol was adapted from (Alvino et al., 2007) Dense medium

777   composition was 0.5% ^{13}C-labeled glucose, 0.5% ^{15}(NH$_4$)$_2$SO$_4$, 0.00145% yeast nitrogen base

778   (YNB), and 1% succinic acid (isotopically-light medium was the same composition with normal

779   glucose and (NH$_4$)$_2$SO$_4$). Cells were cultured in logarithmic phase for at least 10 generations in

780   dense medium with the growth rate assessed for abnormalities. To collect synchronous S-phase

781   cell samples, cultures of ~2.5 x 10^8 cell/mL were arrested with 3 µM α-factor for 1.25 population

782   doublings (approximately 2 hours). Once the cell culture achieved >95% G1 arrest, cells were

783   collected and washed 3 times with isotopically light medium containing α-factor. Cells were

784   resuspended in the original volume of isotopically light medium containing 3 µM α-factor and a

785   100 mL G1 sample was taken for flow cytometry and DNA analysis. Cells were released from

786   G1 into S phase by the addition of 0.15 mg/mL Pronase (EMD Millipore). 100 mL samples

787   were collected and immediately transferred into vessels containing frozen pellets of 40 mL of

788   0.1% sodium azide in 0.2 M EDTA. The entire set of timed samples was collected before

789   pelleting cells, taking a small aliquot for flow cytometry, and transferring the rest of the dry

790   pellet to -20°C for storage until DNA isolation. DNA was extracted using a phenol:chloroform

791   "Smash & Grab" protocol (see above) with an additional chloroform cleanup. Isolated DNA

792   was digested overnight with EcoRI and then centrifuged in CsCl to separate replicated from

793   unreplicated DNA. Cesium chloride gradients were drip-fractionated and the collected samples

794   were analyzed using slot blots and hybridization to microarrays.

795

Flow cytometry:

797   Cells for flow cytometry were fixed in 70% ethanol before processing for flow cytometry. Fixed

798   cells were washed with 50 mM sodium citrate, sonicated, and resuspended in 500 μL 50 mM

799   sodium citrate. RNase A was added to a concentration of 2.5 mg/mL and the samples were

800   incubated for 1 hour at 50°C. Proteinase K (50 μL of 20 mg/mL) was then added and cells were

801   incubated another hour at 50°C before staining with 1X Sytox Green. Cells were analyzed on a

802   BD Canto II flow cytometer and flow cytometry data was analyzed using FlowJo software.

803

804   2D gel electrophoresis:

805   Cells from the 180 rDNA *fob1Δ* strain, the 35 rDNA *fob1Δ* strain, and the 180 rDNA *sir2Δ fob1Δ*

806   strain were grown in logarithmic phase to a culture density of ~2.5 x 10^6 cells/mL. Cultures

807   were then arrested in α-factor for 1.25 doublings before being released into S phase by addition

808   of Pronase (0.15 mg/mL). Samples were collected every 5 minutes: 100 mL for analysis of

809   single-copy genomic origins or 30 mL for analysis of rDNA origins. Collection vessels

810   contained frozen pellets of 0.1% sodium azide in 0.2 M EDTA to halt growth. Cells were

811   washed once with 50 mM EDTA, a small sample taken for flow cytometry, and the remaining

812   dry cell pellets were stored at -20°C until preparation for 2D gel electrophoresis. To extract

813   DNA for 2D gels, cells were embedded in three 90 μL 0.5% SeaPlaque agarose plugs and

814   prepared as CHEF gel plugs. For each 2D gel, each plug was washed 3 x 20 minutes in the

815   appropriate restriction buffer with 1X BSA (100 μg/mL). The solution was then removed and

816   the DNA was digested for 5 hours by addition of 3 μL restriction enzyme directly onto each

817   plug, and then subjected to standard 2D gel electrophoresis methods (Brewer and Fangman,

818   1987), Southern blotted and hybridized for the sequence of interest. Cumulative origin initiation

819   was estimated by integrating the area under the curve generated from plotting "rDNA initiations

820   per cell" across time.

821

822   For 2D gels of cells in hydroxyurea (HU), 20 mL of the culture was transferred to another flask

823   for the "no HU" control to check that cells would have had normal release into S phase.

824   Hydroxyurea was added to the remaining culture to a final concentration of 200 mM and 10

825 minutes later, 0.15 mg/mL Pronase was added to both cultures to release the cells into S phase.

826 Samples were collected every 30 minutes and prepared as above.

827

828 Plasmid maintenance assay:

829 Cells that contained *ARS1* plasmids (Kwan *et al.* 2013) were grown to logarithmic phase in

830 selective medium (YPD + 200 μg/mL G418) and then released into non-selective medium

831 (YPD) for the plasmid maintenance assay. Cells were kept in logarithmic phase growth and

832 samples were collected approximately every 4 hours over the course of 48 hours. The growth

833 rate was monitored to ascertain the number of generations/divisions between samples. DNA was

834 extracted from cells using the "Smash & grab" protocol, digested with XmnI, and run on an

835 agarose gel to resolve the 5.4 kb plasmid *ARS1* fragment from the 3.4 kb genomic *ARS1*

836 fragment (used as a "per cell" loading control). The gel was then Southern blotted and the

837 membrane hybridized to a ^{32}P-labeled *ARS1* fragment. *ARS1* plasmid abundance was assessed

838 through Southern blotting and normalized to the endogenous *ARS1* locus. We quantified the

839 amount of signal from plasmid *ARS1* and genomic *ARS1* for each sample and generated a

840 plasmid maintenance curve for each strain, from which we were able to calculate the rate of

841 plasmid loss per generation and estimate significance using linear regression.

842

843 Spot assays:

844 Cells were grown to log-phase, diluted in sterile water in 3-fold dilutions, and 2.5 μL was

845 spotted onto YPD plates containing either no drug (control), 0.016% methyl methanesulfonate

846 (MMS), or 200 mM hydroxyurea (HU). Plates were scanned after 40-48 hours of growth at

847 30ºC.

848

849 Cycloheximide sensitivity assay:

850 Cells were grown to log phase, upon which 3×10^4 log-phase cells were transferred to each well

851 in a 96-well plate containing 150 μL medium per well and the appropriate concentration of

852   cycloheximide (0-200 ng/mL). Each condition was performed in triplicate and optical densities

853   were measured at 30°C for 48 hours using a Bio-Tek reader. The maximum log-phase growth

854   rate was manually calculated for each well.

855

856   <u>Western blotting:</u>

857   Cells were grown in log phase to ~2.5 x 10^8 cell/mL before α-factor arrest and release. For each

858   strain, 1.5 mL was collected for protein extraction and 1 mL was collected for flow cytometry.

859   Collected cell pellets were resuspended in 200 μL SUMEB buffer (1% SDS, 8 M urea, 10 mM

860   MOPS pH 6.8, 10 mM EDTA, 0.01% bromophenol blue) supplemented with protease inhibitors

861   and 5% β-mercaptoethanol. Glass beads (~100 μL 0.5 mm acid-washed) were added and cells

862   were vortexed for 3 minutes. Lysates were incubated at 65°C for 10 minutes with intermittent

863   shaking and then centrifuged for 5 minutes at 4°C at 20,000 x g. The clarified supernatant was

864   transferred to a new tube and protein concentration was assessed using a Qubit (Thermo Fisher).

865   For each sample, 15 μg of protein was run on a Novex Tris-acetate SDS-PAGE gel and

866   transferred to a nitrocellulose membrane for immunoblotting. HRP-conjugated antibodies

867   against HA (Sigma Aldrich #12013819001) and Pgk1 (Abcam #ab197960) were used in this

868   work.

869

870   <u>Microscopy:</u>

871   Cells were fixed according the protocol described on the Koshland lab web site

872   (http://mcb.berkeley.edu/labs/koshland/Protocols/MICROSCOPY/gfpfix.html): collected cell

873   pellets were resuspended in paraformaldehyde solution (4% paraformaldehyde, 3.4% sucrose)

874   and incubated at room temperature for 15 minutes. Cells were then washed once with

875   KPO$_4$/sorbitol solution and resuspended in 50 μL KPO4/sorbitol solution (0.1 M KPO$_4$ pH 7.5,

876   1.2 M sorbitol) and stored at 4°C until visualization. Before fluorescence microscopy, cells were

877   sonicated and incubated with 0.5 μg/ml DAPI for at least an hour.

878

879

<u>REFERENCES:</u>

881

Abovich, N., Gritz, L., Tung, L., 1985. Effect of RP51 Gene Dosage Alterations on Ribosome Synthesis in Saccharomyces cerevisiae. MOL CELL BIOL 5, 7.

Aldrich, J.C., Maggert, K.A., 2015. Transgenerational inheritance of diet-induced genome rearrangements in Drosophila. PLoS Genet. 11, e1005148. https://doi.org/10.1371/journal.pgen.1005148

Alvino, G.M., Collingwood, D., Murphy, J.M., Delrow, J., Brewer, B.J., Raghuraman, M.K., 2007. Replication in hydroxyurea: it's a matter of time. Mol. Cell. Biol. 27, 6396–6406. https://doi.org/10.1128/MCB.00719-07

Amon, A., 2008. A decade of Cdc14--a personal perspective. Delivered on 9 July 2007 at the 32nd FEBS Congress in Vienna, Austria. FEBS J. 275, 5774–5784. https://doi.org/10.1111/j.1742-4658.2008.06693.x

Barberis, M., Linke, C., Adrover, M.À., González-Novo, A., Lehrach, H., Krobitsch, S., Posas, F., Klipp, E., 2012. Sic1 plays a role in timing and oscillatory behaviour of B-type cyclins. Biotechnol. Adv. 30, 108–130. https://doi.org/10.1016/j.biotechadv.2011.09.004

Bell, S.P., Labib, K., 2016. Chromosome Duplication in Saccharomyces cerevisiae. Genetics 203, 1027–1067. https://doi.org/10.1534/genetics.115.186452

Bénard, M., Lagnel, C., Pierron, G., 1995. Site-specific initiation of DNA replication within the non-transcribed spacer of Physarum rDNA. Nucleic Acids Res. 23, 1447–1453. https://doi.org/10.1093/nar/23.9.1447

Berdougo, E., Nachury, M.V., Jackson, P.K., Jallepalli, P.V., 2008. The nucleolar phosphatase Cdc14B is dispensable for chromosome segregation and mitotic exit in human cells. Cell Cycle Georget. Tex 7, 1184–1190. https://doi.org/10.4161/cc.7.9.5792

Bloom, J., Cross, F.R., 2007. Novel role for Cdc14 sequestration: Cdc14 dephosphorylates factors that promote DNA replication. Mol. Cell. Biol. 27, 842–853. https://doi.org/10.1128/MCB.01069-06

Breitkreutz, A., Choi, H., Sharom, J.R., Boucher, L., Neduva, V., Larsen, B., Lin, Z.-Y., Breitkreutz, B.-J., Stark, C., Liu, G., Ahn, J., Dewar-Darch, D., Reguly, T., Tang, X., Almeida, R., Qin, Z.S., Pawson, T., Gingras, A.-C., Nesvizhskii, A.I., Tyers, M., 2010. A global protein kinase and phosphatase interaction network in yeast. Science 328, 1043–1046. https://doi.org/10.1126/science.1176495

Brewer, B.J., Fangman, W.L., 1994. Initiation preference at a yeast origin of replication. Proc. Natl. Acad. Sci. U. S. A. 91, 3418–3422. https://doi.org/10.1073/pnas.91.8.3418

Brewer, B.J., Fangman, W.L., 1988. A replication fork barrier at the 3' end of yeast ribosomal RNA genes. Cell 55, 637–643. https://doi.org/10.1016/0092-8674(88)90222-x

Brewer, B.J., Fangman, W.L., 1987. The localization of replication origins on ARS plasmids in S. cerevisiae. Cell 51, 463–471. https://doi.org/10.1016/0092-8674(87)90642-8

Brewer, B.J., Lockshon, D., Fangman, W.L., 1992. The arrest of replication forks in the rDNA of yeast occurs independently of transcription. Cell 71, 267–276. https://doi.org/10.1016/0092-8674(92)90355-g

Buchwalter, A., Hetzer, M.W., 2017. Nucleolar expansion and elevated protein translation in premature aging. Nat. Commun. 8, 328. https://doi.org/10.1038/s41467-017-00322-z

Burkhalter, M.D., Sogo, J.M., 2004. rDNA enhancer affects replication initiation and mitotic recombination: Fob1 mediates nucleolytic processing independently of replication. Mol. Cell 15, 409–421. https://doi.org/10.1016/j.molcel.2004.06.024

Chernoff, Y.O., Vincent, A., Liebman, S.W., 1994. Mutations in eukaryotic 18S ribosomal RNA affect translational fidelity and resistance to aminoglycoside antibiotics. EMBO J. 13, 906–913.

Cherry, J.M., Hong, E.L., Amundsen, C., Balakrishnan, R., Binkley, G., Chan, E.T., Christie, K.R., Costanzo, M.C., Dwight, S.S., Engel, S.R., Fisk, D.G., Hirschman, J.E., Hitz, B.C., Karra, K., Krieger, C.J., Miyasato, S.R., Nash, R.S., Park, J., Skrzypek, M.S., Simison, M., Weng, S., Wong, E.D., 2012. Saccharomyces Genome Database: the genomics resource of budding yeast. Nucleic Acids Res. 40, D700-705. https://doi.org/10.1093/nar/gkr1029

Chojnowski, A., Ong, P.F., Foo, M.X.R., Liebl, D., Hor, L.-P., Stewart, C.L., Dreesen, O., 2020. Heterochromatin loss as a determinant of progerin-induced DNA damage in Hutchinson-Gilford Progeria. Aging Cell 19, e13108. https://doi.org/10.1111/acel.13108

Coffman, F.D., He, M., Diaz, M.-L., Cohen, S., 2006. Multiple initiation sites within the human ribosomal RNA gene. Cell Cycle Georget. Tex 5, 1223–1233. https://doi.org/10.4161/cc.5.11.2814

Coffman, F.D., He, M., Diaz, M.-L., Cohen, S., 2005. DNA replication initiates at different sites in early and late S phase within human ribosomal RNA genes. Cell Cycle Georget. Tex 4, 1223–1226. https://doi.org/10.4161/cc.4.9.1961

Collart, C., Allen, G.E., Bradshaw, C.R., Smith, J.C., Zegerman, P., 2013. Titration of four replication factors is essential for the Xenopus laevis midblastula transition. Science 341, 893–896. https://doi.org/10.1126/science.1241530

Concia, L., Brooks, A.M., Wheeler, E., Zynda, G.J., Wear, E.E., LeBlanc, C., Song, J., Lee, T.-J., Pascuzzi, P.E., Martienssen, R.A., Vaughn, M.W., Thompson, W.F., Hanley-Bowdoin, L., 2018. Genome-Wide Analysis of the Arabidopsis Replication Timing Program. Plant Physiol. 176, 2166–2185. https://doi.org/10.1104/pp.17.01537

Conconi, A., Sogo, J.M., Ryan, C.A., 1992. Ribosomal gene clusters are uniquely proportioned between open and closed chromatin structures in both tomato leaf cells and exponentially

growing suspension cultures. Proc. Natl. Acad. Sci. U. S. A. 89, 5256–5260. https://doi.org/10.1073/pnas.89.12.5256

Conconi, A., Widmer, R.M., Koller, T., Sogo, J.M., 1989. Two different chromatin structures coexist in ribosomal RNA genes throughout the cell cycle. Cell 57, 753–761. https://doi.org/10.1016/0092-8674(89)90790-3

Dammann, R., Lucchini, R., Koller, T., Sogo, J.M., 1993. Chromatin structures and transcription of rDNA in yeast Saccharomyces cerevisiae. Nucleic Acids Res. 21, 2331–2338. https://doi.org/10.1093/nar/21.10.2331

D'Amours, D., Amon, A., 2004. At the interface between signaling and executing anaphase-- Cdc14 and the FEAR network. Genes Dev. 18, 2581–2595. https://doi.org/10.1101/gad.1247304

Dauban, L., Kamgoué, A., Wang, R., Léger-Silvestre, I., Beckouët, F., Cantaloube, S., Gadal, O., 2019. Quantification of the dynamic behaviour of ribosomal DNA genes and nucleolus during yeast Saccharomyces cerevisiae cell cycle. J. Struct. Biol. 208, 152–164. https://doi.org/10.1016/j.jsb.2019.08.010

Davé, A., Cooley, C., Garg, M., Bianchi, A., 2014. Protein phosphatase 1 recruitment by Rif1 regulates DNA replication origin firing by counteracting DDK activity. Cell Rep. 7, 53–61. https://doi.org/10.1016/j.celrep.2014.02.019

Delany, M.E., Muscarella, D.E., Bloom, S.E., 1994. Effects of rRNA Gene Copy Number and Nucleolar Variation on Early Development: Inhibition of Gastrulation in rDNA-Deficient Chick Embryo. J. Hered. 85, 211–217. https://doi.org/10.1093/oxfordjournals.jhered.a111437

Egidi, A., Di Felice, F., Camilloni, G., 2020. Saccharomyces cerevisiae rDNA as super-hub: the region where replication, transcription and recombination meet. Cell. Mol. Life Sci. CMLS 77, 4787–4798. https://doi.org/10.1007/s00018-020-03562-3

Eissler, C.L., Mazón, G., Powers, B.L., Savinov, S.N., Symington, L.S., Hall, M.C., 2014. The Cdk/cDc14 module controls activation of the Yen1 holliday junction resolvase to promote genome stability. Mol. Cell 54, 80–93. https://doi.org/10.1016/j.molcel.2014.02.012

Feng, W., Collingwood, D., Boeck, M.E., Fox, L.A., Alvino, G.M., Fangman, W.L., Raghuraman, M.K., Brewer, B.J., 2006. Genomic mapping of single-stranded DNA in hydroxyurea-challenged yeasts identifies origins of replication. Nat. Cell Biol. 8, 148–155. https://doi.org/10.1038/ncb1358

Ferguson, B.M., Fangman, W.L., 1992. A position effect on the time of replication origin activation in yeast. Cell 68, 333–339. https://doi.org/10.1016/0092-8674(92)90474-q

Foss, E.J., Gatbonton-Schwager, T., Thiesen, A.H., Taylor, E., Soriano, R., Lao, U., MacAlpine, D.M., Bedalov, A., 2019. Sir2 suppresses transcription-mediated displacement of Mcm2-7 replicative helicases at the ribosomal DNA repeats. PLoS Genet. 15, e1008138. https:// doi.org/10.1371/journal.pgen.1008138

Foss, E.J., Lao, U., Dalrymple, E., Adrianse, R.L., Loe, T., Bedalov, A., 2017. SIR2 suppresses replication gaps and genome instability by balancing replication between repetitive and unique sequences. Proc. Natl. Acad. Sci. U. S. A. 114, 552–557. https://doi.org/10.1073/pnas.1614781114

French, S.L., Osheim, Y.N., Cioci, F., Nomura, M., Beyer, A.L., 2003. In Exponentially Growing Saccharomyces cerevisiae Cells, rRNA Synthesis Is Determined by the Summed RNA Polymerase I Loading Rate Rather than by the Number of Active Genes. Mol. Cell. Biol. 23, 1558–1568. https://doi.org/10.1128/MCB.23.5.1558-1568.2003

Friedel, A.M., Pike, B.L., Gasser, S.M., 2009. ATR/Mec1: coordinating fork stability and repair. Curr. Opin. Cell Biol. 21, 237–244. https://doi.org/10.1016/j.ceb.2009.01.017

Friedman, K.L., Brewer, B.J., Fangman, W.L., 1997. Replication profile of Saccharomyces cerevisiae chromosome VI. Genes Cells Devoted Mol. Cell. Mech. 2, 667–678. https://doi.org/10.1046/j.1365-2443.1997.1520350.x

Gibbons, J.G., Branco, A.T., Yu, S., Lemos, B., 2014. Ribosomal DNA copy number is coupled with gene expression variation and mitochondrial abundance in humans. Nat. Commun. 5, 4850. https://doi.org/10.1038/ncomms5850

Hafner, L., Lezaja, A., Zhang, X., Lemmens, L., Shyian, M., Albert, B., Follonier, C., Nunes, J.M., Lopes, M., Shore, D., Mattarocci, S., 2018. Rif1 Binding and Control of Chromosome-Internal DNA Replication Origins Is Limited by Telomere Sequestration. Cell Rep. 23, 983–992. https://doi.org/10.1016/j.celrep.2018.03.113

Hartwell, L.H., Culotti, J., Pringle, J.R., Reid, B.J., 1974. Genetic control of the cell division cycle in yeast. Science 183, 46–51. https://doi.org/10.1126/science.183.4120.46

Hennessy, K.M., Lee, A., Chen, E., Botstein, D., 1991. A group of interacting yeast DNA replication genes. Genes Dev. 5, 958–969. https://doi.org/10.1101/gad.5.6.958

Hiraga, S.-I., Alvino, G.M., Chang, F., Lian, H.-Y., Sridhar, A., Kubota, T., Brewer, B.J., Weinreich, M., Raghuraman, M.K., Donaldson, A.D., 2014. Rif1 controls DNA replication by directing Protein Phosphatase 1 to reverse Cdc7-mediated phosphorylation of the MCM complex. Genes Dev. 28, 372–383. https://doi.org/10.1101/gad.231258.113

Ho, B., Baryshnikova, A., Brown, G.W., 2018. Unification of Protein Abundance Datasets Yields a Quantitative Saccharomyces cerevisiae Proteome. Cell Syst. 6, 192-205.e3. https://doi.org/10.1016/j.cels.2017.12.004

Hoang, M.L., Leon, R.P., Pessoa-Brandao, L., Hunt, S., Raghuraman, M.K., Fangman, W.L., Brewer, B.J., Sclafani, R.A., 2007. Structural changes in Mcm5 protein bypass Cdc7-Dbf4 function and reduce replication origin efficiency in Saccharomyces cerevisiae. Mol. Cell. Biol. 27, 7594–7602. https://doi.org/10.1128/MCB.00997-07

Hoggard, T., Müller, C.A., Nieduszynski, C.A., Weinreich, M., Fox, C.A., 2020. Sir2 mitigates an intrinsic imbalance in origin licensing efficiency between early- and late-replicating euchromatin. Proc. Natl. Acad. Sci. U. S. A. 117, 14314–14321. https://doi.org/10.1073/pnas.2004664117

Hoggard, T.A., Chang, F., Perry, K.R., Subramanian, S., Kenworthy, J., Chueng, J., Shor, E., Hyland, E.M., Boeke, J.D., Weinreich, M., Fox, C.A., 2018. Yeast heterochromatin regulators Sir2 and Sir3 act directly at euchromatic DNA replication origins. PLoS Genet. 14, e1007418. https://doi.org/10.1371/journal.pgen.1007418

Huang, J., Brito, I.L., Villén, J., Gygi, S.P., Amon, A., Moazed, D., 2006. Inhibition of homologous recombination by a cohesin-associated clamp complex recruited to the rDNA recombination enhancer. Genes Dev. 20, 2887–2901. https://doi.org/10.1101/gad.1472706

Huang, J., Moazed, D., 2003. Association of the RENT complex with nontranscribed and coding regions of rDNA and a regional requirement for the replication fork block protein Fob1 in rDNA silencing. Genes Dev. 17, 2162–2176. https://doi.org/10.1101/gad.1108403

Huh, W.-K., Falvo, J.V., Gerke, L.C., Carroll, A.S., Howson, R.W., Weissman, J.S., O'Shea, E.K., 2003. Global analysis of protein localization in budding yeast. Nature 425, 686–691. https://doi.org/10.1038/nature02026

Hyrien, O., Méchali, M., 1992. Plasmid replication in Xenopus eggs and egg extracts: a 2D gel electrophoretic analysis. Nucleic Acids Res. 20, 1463–1469. https://doi.org/10.1093/nar/20.7.1463

Ide, S., Miyazaki, T., Maki, H., Kobayashi, T., 2010. Abundance of ribosomal RNA gene copies maintains genome integrity. Science 327, 693–696. https://doi.org/10.1126/science.1179044

Ide, S., Watanabe, K., Watanabe, H., Shirahige, K., Kobayashi, T., Maki, H., 2007. Abnormality in initiation program of DNA replication is monitored by the highly repetitive rRNA gene array on chromosome XII in budding yeast. Mol. Cell. Biol. 27, 568–578. https://doi.org/10.1128/MCB.00731-06

Kaiser, B.K., Nachury, M.V., Gardner, B.E., Jackson, P.K., 2004. Xenopus Cdc14 alpha/beta are localized to the nucleolus and centrosome and are required for embryonic cell division. BMC Cell Biol. 5, 27. https://doi.org/10.1186/1471-2121-5-27

Kaneva, I.N., Sudbery, I.M., Dickman, M.J., Sudbery, P.E., 2019. Proteins that physically interact with the phosphatase Cdc14 in Candida albicans have diverse roles in the cell cycle. Sci. Rep. 9, 6258. https://doi.org/10.1038/s41598-019-42530-1

Khmelinskii, A., Lawrence, C., Roostalu, J., Schiebel, E., 2007. Cdc14-regulated midzone assembly controls anaphase B. J. Cell Biol. 177, 981–993. https://doi.org/10.1083/jcb.200702145

Kim, Y.-H., Ishikawa, D., Ha, H.P., Sugiyama, M., Kaneko, Y., Harashima, S., 2006. Chromosome XII context is important for rDNA function in yeast. Nucleic Acids Res. 34, 2914–2924. https://doi.org/10.1093/nar/gkl293

Kobayashi, T., 2003. The replication fork barrier site forms a unique structure with Fob1p and inhibits the replication fork. Mol. Cell. Biol. 23, 9178–9188. https://doi.org/10.1128/mcb.23.24.9178-9188.2003

Kobayashi, T., Heck, D.J., Nomura, M., Horiuchi, T., 1998. Expansion and contraction of ribosomal DNA repeats in Saccharomyces cerevisiae: requirement of replication fork blocking (Fob1) protein and the role of RNA polymerase I. Genes Dev. 12, 3821–3830. https://doi.org/10.1101/gad.12.24.3821

Kobayashi, T., Nomura, M., Horiuchi, T., 2001. Identification of DNA cis elements essential for expansion of ribosomal DNA repeats in Saccharomyces cerevisiae. Mol. Cell. Biol. 21, 136–147. https://doi.org/10.1128/MCB.21.1.136-147.2001

Krawczyk, C., Dion, V., Schär, P., Fritsch, O., 2014. Reversible Top1 cleavage complexes are stabilized strand-specifically at the ribosomal replication fork barrier and contribute to ribosomal DNA stability. Nucleic Acids Res. 42, 4985–4995. https://doi.org/10.1093/nar/gku148

Kulak, N.A., Pichler, G., Paron, I., Nagaraj, N., Mann, M., 2014. Minimal, encapsulated proteomic-sample processing applied to copy-number estimation in eukaryotic cells. Nat. Methods 11, 319–324. https://doi.org/10.1038/nmeth.2834

Kwan, E.X., Foss, E.J., Tsuchiyama, S., Alvino, G.M., Kruglyak, L., Kaeberlein, M., Raghuraman, M.K., Brewer, B.J., Kennedy, B.K., Bedalov, A., 2013. A natural polymorphism in rDNA replication origins links origin activation with calorie restriction and lifespan. PLoS Genet. 9, e1003329. https://doi.org/10.1371/journal.pgen.1003329

Kwan, E.X., Wang, X.S., Amemiya, H.M., Brewer, B.J., Raghuraman, M.K., 2016. rDNA Copy Number Variants Are Frequent Passenger Mutations in Saccharomyces cerevisiae Deletion Collections and de Novo Transformants. G3 Bethesda Md 6, 2829–2838. https://doi.org/10.1534/g3.116.030296

Labit, H., Perewoska, I., Germe, T., Hyrien, O., Marheineke, K., 2008. DNA replication timing is deterministic at the level of chromosomal domains but stochastic at the level of replicons in Xenopus egg extracts. Nucleic Acids Res. 36, 5623–5634. https://doi.org/10.1093/nar/gkn533

Linskens, M.H., Huberman, J.A., 1988. Organization of replication of ribosomal DNA in Saccharomyces cerevisiae. Mol. Cell. Biol. 8, 4927–4935. https://doi.org/10.1128/mcb.8.11.4927

Little, R.D., Platt, T.H., Schildkraut, C.L., 1993. Initiation and termination of DNA replication in human rRNA genes. Mol. Cell. Biol. 13, 6600–6613. https://doi.org/10.1128/mcb.13.10.6600

Longtine, M.S., McKenzie, A., Demarini, D.J., Shah, N.G., Wach, A., Brachat, A., Philippsen, P., Pringle, J.R., 1998. Additional modules for versatile and economical PCR-based gene deletion and modification in Saccharomyces cerevisiae. Yeast Chichester Engl. 14, 953–961. https://doi.org/10.1002/(SICI)1097-0061(199807)14:10<953::AID-YEA293>3.0.CO;2-U

López-estraño, C., Schvartzman, J.B., Krimer, D.B., Hernández, P., 1998. Co-localization of polar replication fork barriers and rRNA transcription terminators in mouse rDNA. J. Mol. Biol. 277, 249–256. https://doi.org/10.1006/jmbi.1997.1607

Lu, K.L., Nelson, J.O., Watase, G.J., Warsinger-Pepe, N., Yamashita, Y.M., 2018. Transgenerational dynamics of rDNA copy number in Drosophila male germline stem cells. eLife 7. https://doi.org/10.7554/eLife.32421

Lynch, K.L., Alvino, G.M., Kwan, E.X., Brewer, B.J., Raghuraman, M.K., 2019. The effects of manipulating levels of replication initiation factors on origin firing efficiency in yeast. PLoS Genet. 15, e1008430. https://doi.org/10.1371/journal.pgen.1008430

Maine, G.T., Sinha, P., Tye, B.K., 1984. Mutants of S. cerevisiae defective in the maintenance of minichromosomes. Genetics 106, 365–385.

Maiti, A.K., Sinha, P., 1992. The mcm2 mutation of yeast affects replication, rather than segregation or amplification of the two micron plasmid. J. Mol. Biol. 224, 545–558. https://doi.org/10.1016/0022-2836(92)90543-s

Mantiero, D., Mackenzie, A., Donaldson, A., Zegerman, P., 2011. Limiting replication initiation factors execute the temporal programme of origin firing in budding yeast. EMBO J. 30, 4805–4814. https://doi.org/10.1038/emboj.2011.404

Manzano-López, J., Monje-Casas, F., 2020. The Multiple Roles of the Cdc14 Phosphatase in Cell Cycle Control. Int. J. Mol. Sci. 21. https://doi.org/10.3390/ijms21030709

Masumoto, H., Muramatsu, S., Kamimura, Y., Araki, H., 2002. S-Cdk-dependent phosphorylation of Sld2 essential for chromosomal DNA replication in budding yeast. Nature 415, 651–655. https://doi.org/10.1038/nature713

Mattarocci, S., Shyian, M., Lemmens, L., Damay, P., Altintas, D.M., Shi, T., Bartholomew, C.R., Thomä, N.H., Hardy, C.F.J., Shore, D., 2014. Rif1 controls DNA replication timing in yeast through the PP1 phosphatase Glc7. Cell Rep. 7, 62–69. https://doi.org/10.1016/j.celrep.2014.03.010

McStay, B., Grummt, I., 2008. The Epigenetics of rRNA Genes: From Molecular to Chromosome Biology. Annu. Rev. Cell Dev. Biol. 24, 131–157. https://doi.org/10.1146/annurev.cellbio.24.110707.175259

Michel, A.H., Kornmann, B., Dubrana, K., Shore, D., 2005. Spontaneous rDNA copy number variation modulates Sir2 levels and epigenetic gene silencing. Genes Dev. 19, 1199–1210. https://doi.org/10.1101/gad.340205

Miller, C.A., Kowalski, D., 1993. cis-acting components in the replication origin from ribosomal DNA of Saccharomyces cerevisiae. Mol. Cell. Biol. 13, 5360–5369. https://doi.org/10.1128/mcb.13.9.5360

Minchell, N.E., Keszthelyi, A., Baxter, J., 2020. Cohesin Causes Replicative DNA Damage by Trapping DNA Topological Stress. Mol. Cell 78, 739-751.e8. https://doi.org/10.1016/j.molcel.2020.03.013

Mohan, J., Ritossa, F.M., 1970. Regulation of ribosomal RNA synthesis and its bearing on the bobbed phenotype in Drosophila melanogaster. Dev. Biol. 22, 495–512. https://doi.org/10.1016/0012-1606(70)90165-x

Mohl, D.A., Huddleston, M.J., Collingwood, T.S., Annan, R.S., Deshaies, R.J., 2009. Dbf2-Mob1 drives relocalization of protein phosphatase Cdc14 to the cytoplasm during exit from mitosis. J Cell Biol 184, 527–539. https://doi.org/10.1083/jcb.200812022

Morton, E.A., Hall, A.N., Kwan, E., Mok, C., Queitsch, K., Nandakumar, V., Stamatoyannopoulos, J., Brewer, B.J., Waterston, R., Queitsch, C., 2020. Challenges and Approaches to Genotyping Repetitive DNA. G3 Bethesda Md 10, 417–430. https://doi.org/10.1534/g3.119.400771

Nelson, J.O., Watase, G.J., Warsinger-Pepe, N., Yamashita, Y.M., 2019. Mechanisms of rDNA Copy Number Maintenance. Trends Genet. TIG 35, 734–742. https://doi.org/10.1016/j.tig.2019.07.006

Nieduszynski, C.A., Hiraga, S., Ak, P., Benham, C.J., Donaldson, A.D., 2007. OriDB: a DNA replication origin database. Nucleic Acids Res. 35, D40-46. https://doi.org/10.1093/nar/gkl758

Paredes, S., Branco, A.T., Hartl, D.L., Maggert, K.A., Lemos, B., 2011. Ribosomal DNA deletions modulate genome-wide gene expression: "rDNA-sensitive" genes and natural variation. PLoS Genet. 7, e1001376. https://doi.org/10.1371/journal.pgen.1001376

Parks, M.M., Kurylo, C.M., Dass, R.A., Bojmar, L., Lyden, D., Vincent, C.T., Blanchard, S.C., 2018. Variant ribosomal RNA alleles are conserved and exhibit tissue-specific expression. Sci. Adv. 4, eaao0665. https://doi.org/10.1126/sciadv.aao0665

Paulovich, A.G., Hartwell, L.H., 1995. A checkpoint regulates the rate of progression through S phase in S. cerevisiae in response to DNA damage. Cell 82, 841–847. https://doi.org/10.1016/0092-8674(95)90481-6

Picart-Picolo, A., Grob, S., Picault, N., Franek, M., Llauro, C., Halter, T., Maier, T.R., Jobet, E., Descombin, J., Zhang, P., Paramasivan, V., Baum, T.J., Navarro, L., Dvořáčková, M., Mirouze, M., Pontvianne, F., 2020. Large tandem duplications affect gene expression, 3D organization, and plant-pathogen response. Genome Res. 30, 1583–1592. https://doi.org/10.1101/gr.261586.120

Radford, A., 1991. Methods in yeast genetics — A laboratory course manual by M Rose, F Winston and P Hieter. pp 198. Cold Spring Harbor Laboratory Press, Cold Spring Harbor, New York. 1990. $34 ISBN 0-87969-354-1. Biochem. Educ. 19, 101–102. https://doi.org/10.1016/0307-4412(91)90039-B

Raghuraman, M.K., Winzeler, E.A., Collingwood, D., Hunt, S., Wodicka, L., Conway, A., Lockhart, D.J., Davis, R.W., Brewer, B.J., Fangman, W.L., 2001. Replication dynamics of the yeast genome. Science 294, 115–121. https://doi.org/10.1126/science.294.5540.115

Ritossa, F.M., Atwood, K.C., 1966. Unequal proportions of DNA complementary to ribosomal RNA in males and females of Drosophila simulans. Proc. Natl. Acad. Sci. U. S. A. 56, 496–499.

43

Rosado, I.V., Kressler, D., de la Cruz, J., 2007. Functional analysis of Saccharomyces cerevisiae ribosomal protein Rpl3p in ribosome synthesis. Nucleic Acids Res. 35, 4203–4213. https://doi.org/10.1093/nar/gkm388

Saito, R.M., Perreault, A., Peach, B., Satterlee, J.S., van den Heuvel, S., 2004. The CDC-14 phosphatase controls developmental cell-cycle arrest in C. elegans. Nat. Cell Biol. 6, 777–783. https://doi.org/10.1038/ncb1154

Saka, K., Ide, S., Ganley, A.R.D., Kobayashi, T., 2013. Cellular senescence in yeast is regulated by rDNA noncoding transcription. Curr. Biol. CB 23, 1794–1798. https://doi.org/10.1016/j.cub.2013.07.048

Salim, D., Bradford, W.D., Freeland, A., Cady, G., Wang, J., Pruitt, S.C., Gerton, J.L., 2017. DNA replication stress restricts ribosomal DNA copy number. PLoS Genet. 13, e1007006. https://doi.org/10.1371/journal.pgen.1007006

Salim, D., Bradford, W.D., Rubinstein, B., Gerton, J.L., 2021. DNA replication, transcription, and H3K56 acetylation regulate copy number and stability at tandem repeats. G3 Bethesda Md. https://doi.org/10.1093/g3journal/jkab082

Sanchez, J.C., Kwan, E.X., Pohl, T.J., Amemiya, H.M., Raghuraman, M.K., Brewer, B.J., 2017. Defective replication initiation results in locus specific chromosome breakage and a ribosomal RNA deficiency in yeast. PLoS Genet. 13, e1007041. https://doi.org/10.1371/journal.pgen.1007041

Santocanale, C., Diffley, J.F., 1998. A Mec1- and Rad53-dependent checkpoint controls late-firing origins of DNA replication. Nature 395, 615–618. https://doi.org/10.1038/27001

Schübeler, D., Scalzo, D., Kooperberg, C., van Steensel, B., Delrow, J., Groudine, M., 2002. Genome-wide DNA replication profile for Drosophila melanogaster: a link between transcription and replication timing. Nat. Genet. 32, 438–442. https://doi.org/10.1038/ng1005

Schwob, E., Böhm, T., Mendenhall, M.D., Nasmyth, K., 1994. The B-type cyclin kinase inhibitor p40SIC1 controls the G1 to S transition in S. cerevisiae. Cell 79, 233–244. https://doi.org/10.1016/0092-8674(94)90193-7

Schwob, E., Nasmyth, K., 1993. CLB5 and CLB6, a new pair of B cyclins involved in DNA replication in Saccharomyces cerevisiae. Genes Dev. 7, 1160–1175. https://doi.org/10.1101/gad.7.7a.1160

Segurado, M., Tercero, J.A., 2009. The S-phase checkpoint: targeting the replication fork. Biol. Cell 101, 617–627. https://doi.org/10.1042/BC20090053

Shima, N., Alcaraz, A., Liachko, I., Buske, T.R., Andrews, C.A., Munroe, R.J., Hartford, S.A., Tye, B.K., Schimenti, J.C., 2007. A viable allele of Mcm4 causes chromosome instability and mammary adenocarcinomas in mice. Nat. Genet. 39, 93–98. https://doi.org/10.1038/ng1936

Shimada, K., Pasero, P., Gasser, S.M., 2002. ORC and the intra-S-phase checkpoint: a threshold regulates Rad53p activation in S phase. Genes Dev. 16, 3236–3252. https://doi.org/10.1101/gad.239802

Shou, W., Seol, J.H., Shevchenko, A., Baskerville, C., Moazed, D., Chen, Z.W., Jang, J., Shevchenko, A., Charbonneau, H., Deshaies, R.J., 1999. Exit from mitosis is triggered by Tem1-dependent release of the protein phosphatase Cdc14 from nucleolar RENT complex. Cell 97, 233–244. https://doi.org/10.1016/s0092-8674(00)80733-3

Shyian, M., Mattarocci, S., Albert, B., Hafner, L., Lezaja, A., Costanzo, M., Boone, C., Shore, D., 2016. Budding Yeast Rif1 Controls Genome Integrity by Inhibiting rDNA Replication. PLoS Genet. 12, e1006414. https://doi.org/10.1371/journal.pgen.1006414

Smith, J.S., Boeke, J.D., 1997. An unusual form of transcriptional silencing in yeast ribosomal DNA. Genes Dev. 11, 241–254. https://doi.org/10.1101/gad.11.2.241

Stegmeier, F., Huang, J., Rahal, R., Zmolik, J., Moazed, D., Amon, A., 2004. The replication fork block protein Fob1 functions as a negative regulator of the FEAR network. Curr. Biol. CB 14, 467–480. https://doi.org/10.1016/j.cub.2004.03.009

Stinchcomb, D.T., Struhl, K., Davis, R.W., 1979. Isolation and characterisation of a yeast chromosomal replicator. Nature 282, 39–43. https://doi.org/10.1038/282039a0

Storici, F., Oberto, J., Bruschi, C.V., 1995. The CDC6 gene is required for centromeric, episomal, and 2-microns plasmid stability in the yeast Saccharomyces cerevisiae. Plasmid 34, 184–197. https://doi.org/10.1006/plas.1995.0004

Thaminy, S., Newcomb, B., Kim, J., Gatbonton, T., Foss, E., Simon, J., Bedalov, A., 2007. Hst3 is regulated by Mec1-dependent proteolysis and controls the S phase checkpoint and sister chromatid cohesion by deacetylating histone H3 at lysine 56. J. Biol. Chem. 282, 37805–37814. https://doi.org/10.1074/jbc.M706384200

Thompson, O., Edgley, M., Strasbourger, P., Flibotte, S., Ewing, B., Adair, R., Au, V., Chaudhry, I., Fernando, L., Hutter, H., Kieffer, A., Lau, J., Lee, N., Miller, A., Raymant, G., Shen, B., Shendure, J., Taylor, J., Turner, E.H., Hillier, L.W., Moerman, D.G., Waterston, R.H., 2013. The million mutation project: a new approach to genetics in Caenorhabditis elegans. Genome Res. 23, 1749–1762. https://doi.org/10.1101/gr.157651.113

Trabold, P.A., Weinberger, M., Feng, L., Burhans, W.C., 2005. Activation of budding yeast replication origins and suppression of lethal DNA damage effects on origin function by ectopic expression of the co-chaperone protein Mge1. J. Biol. Chem. 280, 12413–12421. https://doi.org/10.1074/jbc.M411327200

Tsuchiyama, S., Kwan, E., Dang, W., Bedalov, A., Kennedy, B.K., 2013. Sirtuins in yeast: phenotypes and tools. Methods Mol. Biol. Clifton NJ 1077, 11–37. https://doi.org/10.1007/978-1-62703-637-5_2

Tye, B.K., 1999. Minichromosome maintenance as a genetic assay for defects in DNA replication. Methods San Diego Calif 18, 329–334. https://doi.org/10.1006/meth.1999.0793

Verma, R., Annan, R.S., Huddleston, M.J., Carr, S.A., Reynard, G., Deshaies, R.J., 1997. Phosphorylation of Sic1p by G1 Cdk required for its degradation and entry into S phase. Science 278, 455–460. https://doi.org/10.1126/science.278.5337.455

Villoria, M.T., Ramos, F., Dueñas, E., Faull, P., Cutillas, P.R., Clemente-Blanco, A., 2017. Stabilization of the metaphase spindle by Cdc14 is required for recombinational DNA repair. EMBO J. 36, 79–101. https://doi.org/10.15252/embj.201593540

Visintin, R., Craig, K., Hwang, E.S., Prinz, S., Tyers, M., Amon, A., 1998. The phosphatase Cdc14 triggers mitotic exit by reversal of Cdk-dependent phosphorylation. Mol. Cell 2, 709–718. https://doi.org/10.1016/s1097-2765(00)80286-5

Visintin, R., Hwang, E.S., Amon, A., 1999. Cfi1 prevents premature exit from mitosis by anchoring Cdc14 phosphatase in the nucleolus. Nature 398, 818–823. https://doi.org/10.1038/19775

Wang, M., Lemos, B., 2017. Ribosomal DNA copy number amplification and loss in human cancers is linked to tumor genetic context, nucleolus activity, and proliferation. PLoS Genet. 13, e1006994. https://doi.org/10.1371/journal.pgen.1006994

Ward, T.R., Hoang, M.L., Prusty, R., Lau, C.K., Keil, R.L., Fangman, W.L., Brewer, B.J., 2000. Ribosomal DNA replication fork barrier and HOT1 recombination hot spot: shared sequences but independent activities. Mol. Cell. Biol. 20, 4948–4957. https://doi.org/10.1128/mcb.20.13.4948-4957.2000

Woolford, J.L., Baserga, S.J., 2013. Ribosome biogenesis in the yeast Saccharomyces cerevisiae. Genetics 195, 643–681. https://doi.org/10.1534/genetics.113.153197

Wu, J., Cho, H.P., Rhee, D.B., Johnson, D.K., Dunlap, J., Liu, Y., Wang, Y., 2008. Cdc14B depletion leads to centriole amplification, and its overexpression prevents unscheduled centriole duplication. J. Cell Biol. 181, 475–483. https://doi.org/10.1083/jcb.200710127

Xu, B., Li, H., Perry, J.M., Singh, V.P., Unruh, J., Yu, Z., Zakari, M., McDowell, W., Li, L., Gerton, J.L., 2017. Ribosomal DNA copy number loss and sequence variation in cancer. PLoS Genet. 13, e1006771. https://doi.org/10.1371/journal.pgen.1006771Xue, Y., Rushton, M.D., Maringele, L., 2011. A novel checkpoint and RPA inhibitory pathway regulated by Rif1. PLoS Genet. 7, e1002417. https://doi.org/10.1371/journal.pgen.1002417

Yabuki, N., Terashima, H., Kitada, K., 2002. Mapping of early firing origins on a replication profile of budding yeast. Genes Cells Devoted Mol. Cell. Mech. 7, 781–789. https://doi.org/10.1046/j.1365-2443.2002.00559.x

Ye, J., Eickbush, T.H., 2006. Chromatin structure and transcription of the R1- and R2-inserted rRNA genes of Drosophila melanogaster. Mol. Cell. Biol. 26, 8781–8790. https://doi.org/10.1128/MCB.01409-06

Yellman, C.M., Roeder, G.S., 2015. Cdc14 Early Anaphase Release, FEAR, Is Limited to the Nucleus and Dispensable for Efficient Mitotic Exit. PloS One 10, e0128604. https://doi.org/10.1371/journal.pone.0128604

Yoshida, K., Bacal, J., Desmarais, D., Padioleau, I., Tsaponina, O., Chabes, A., Pantesco, V., Dubois, E., Parrinello, H., Skrzypczak, M., Ginalski, K., Lengronne, A., Pasero, P., 2014. The histone deacetylases sir2 and rpd3 act on ribosomal DNA to control the replication program in budding yeast. Mol. Cell 54, 691–697. https://doi.org/10.1016/j.molcel.2014.04.032

Yoshida, K., Poveda, A., Pasero, P., 2013. Time to be versatile: regulation of the replication timing program in budding yeast. J. Mol. Biol. 425, 4696–4705. https://doi.org/10.1016/j.jmb.2013.09.020

882